Targeting iron homeostasis induces cellular differentiation and synergizes with differentiating agents in acute myeloid leukemia

Celine Callens,[1,2] Séverine Coulon,[1,2] Jerome Naudin,[1,2,3,4] Isabelle Radford-Weiss,[2,5] Nicolas Boissel,[4,9] Emmanuel Raffoux,[4,9] Pamella Huey Mei Wang,[3,4] Saurabh Agarwal,[3,4] Houda Tamouza,[3,4] Etienne Paubelle,[1,2] Vahid Asnafi,[1,2,6] Jean-Antoine Ribeil,[1,2] Philippe Dessen,[10] Danielle Canioni,[2,7] Olivia Chandesris,[2,8] Marie Therese Rubio,[2,8] Carole Beaumont,[4,11] Marc Benhamou,[3,4] Hervé Dombret,[4,9] Elizabeth Macintyre,[1,2,6] Renato C. Monteiro,[3,4] Ivan C. Moura,[3,4] and Olivier Hermine[1,2,8]

[1]Centre National de la Recherche Scientifique UMR 8147, Paris 75015, France
[2]Faculté de Médecine, Université René Descartes Paris V, Institut Fédératif Necker, Paris 75015, France
[3]Institut National de la Santé et de la Recherche Médicale (INSERM), U699, Paris 75018, France
[4]Faculté de Médecine, Université Denis Diderot Paris VII, Paris 75018, France
[5]Laboratoire de cytogénétique, [6]Laboratoire d'Hématologie, [7]Service d'Anatomo-Pathologie, and [8]Service d'Hématologie, Hôpital Necker-Enfants Malades, Assistance Publique Hôpitaux de Paris (AP-HP), Paris 75015, France
[9]Service d'Hématologie, Hôpital Saint-Louis, AP-HP, Paris 75010, France
[10]Unité de Génomique Fonctionnelle, Institut Gustave Roussy, Villejuif 94800, France
[11]INSERM U773, Centre de Recherche Biomédicale Bichat Beaujon CRB3, Paris 75018, France

Differentiating agents have been proposed to overcome the impaired cellular differentiation in acute myeloid leukemia (AML). However, only the combinations of all-trans retinoic acid or arsenic trioxide with chemotherapy have been successful, and only in treating acute promyelocytic leukemia (also called AML3). We show that iron homeostasis is an effective target in the treatment of AML. Iron chelating therapy induces the differentiation of leukemia blasts and normal bone marrow precursors into monocytes/macrophages in a manner involving modulation of reactive oxygen species expression and the activation of mitogen-activated protein kinases (MAPKs). 30% of the genes most strongly induced by iron deprivation are also targeted by vitamin D3 (VD), a well known differentiating agent. Iron chelating agents induce expression and phosphorylation of the VD receptor (VDR), and iron deprivation and VD act synergistically. VD magnifies activation of MAPK JNK and the induction of VDR target genes. When used to treat one AML patient refractory to chemotherapy, the combination of iron-chelating agents and VD resulted in reversal of pancytopenia and in blast differentiation. We propose that iron availability modulates myeloid cell commitment and that targeting this cellular differentiation pathway together with conventional differentiating agents provides new therapeutic modalities for AML.

CORRESPONDENCE
Olivier Hermine:
olivier.hermine@nck.aphp.fr
OR
Ivan Cruz Moura:
ivan.moura@inserm.fr

Abbreviations used: AML, acute myeloid leukemia; APL, acute promyelocytic leukemia; ATO, arsenic trioxide; ATRA, all-trans retinoic acid; CI, combination index; DFO, deferoxamine; DFX, deferasirox; DHE, dihydroethidium; DHR123, dihydrorhodamine 123; FAB, French-American-British; LIP, labile iron pool; MAPK, mitogen-activated protein kinase; MDS, myelodysplastic syndrome; MFI, mean fluorescence intensity; MGG, May Grünwald Giemsa; miRNA, micro RNA; mRNA, messenger RNA; NAC, *N*-acetyl-L-cysteine; PDTC, pyrrolidine dithiocarbamate; PI, propidium iodide; ROS, reactive oxygen species; SCF, stem cell factor; VD, vitamin D3; VDR, VD receptor.

Acute myeloid leukemia (AML) is a heterogeneous malignant disorder originating from mutations in progenitor cells that lead to the unrestrained proliferation of undifferentiated myeloblasts (Löwenberg et al., 1999). There is a general consensus that the molecular events leading to AML leukemogenesis occur as a multistep process (Kelly and Gilliland, 2002; Gilliland et al., 2004). Those events are broadly classified into two groups: gene alterations that confer a proliferative and/or survival advantage to hematopoietic progenitors (e.g., *RAS*,

I.C. Moura and O. Hermine contributed equally to this paper.
C. Callens' present adress is Laboratoire d'Hématologie, Hôpital Necker-Enfants Malades, AP-HP, Paris, 75015 France.

The Rockefeller University Press $30.00
J. Exp. Med. Vol. 207 No. 4 731-750
www.jem.org/cgi/doi/10.1084/jem.20091488

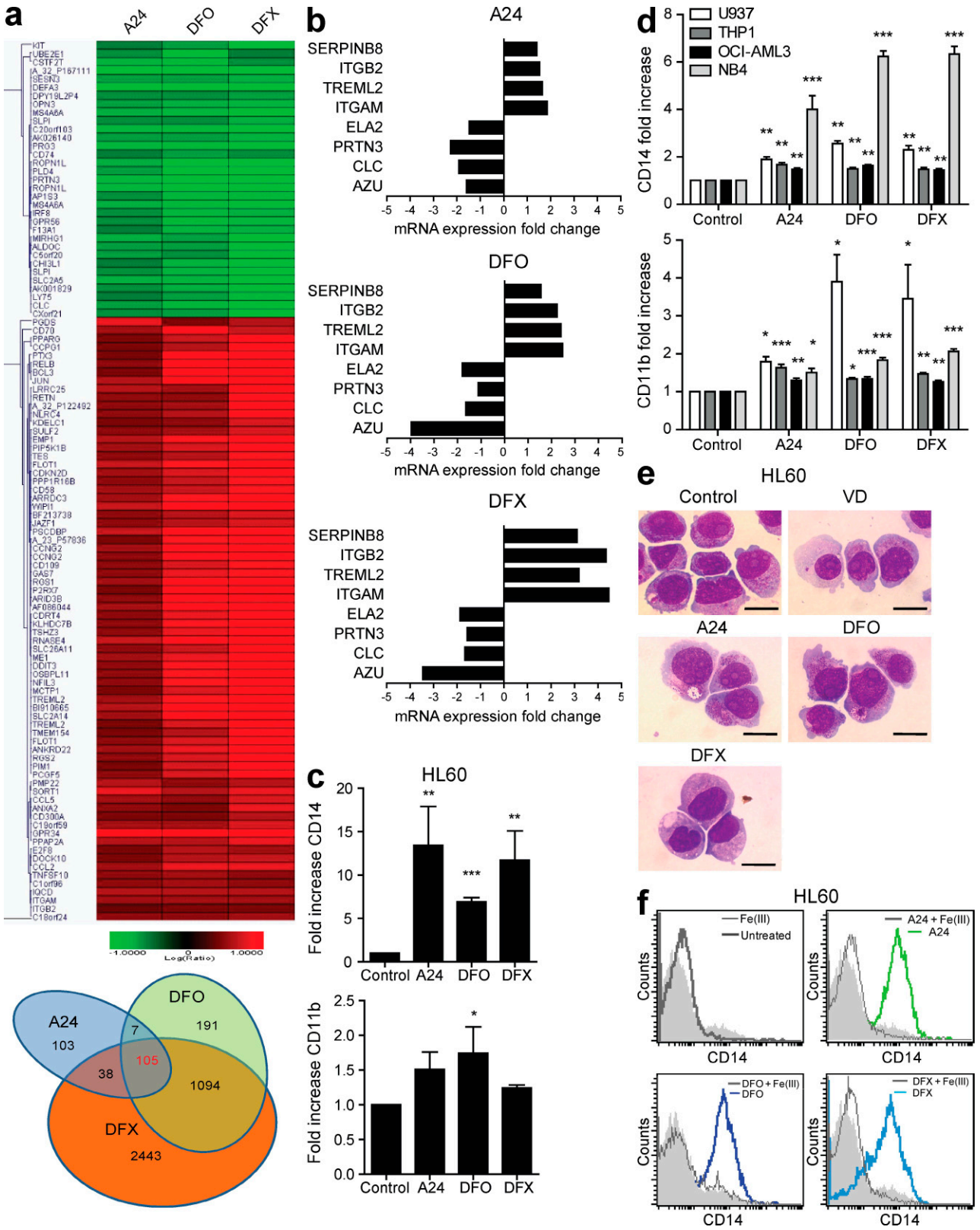

Figure 1. Iron deprivation induces monocyte differentiation of AML cells. (a) Unsupervised microarray analysis of HL60 cells after a 48-h exposure to 10 µg/ml of anti-TfR1 antibody (mAb A24), 5 µM DFO, or 3 µM DFX. The color intensity represents the ratio of expression in drug-treated compared with control cells. The relative overexpression and underexpression compared with controls are shown in red and green, respectively (top). A Venn diagram of genes induced by iron deprivation (bottom) shows that only a subset of genes (105) have a shared altered expression between the

FLT3, or *KIT* mutations) and gene alterations/point mutations in transcription factors or transcriptional coactivators (e.g., *CEBPα* and *NPM1*) that affect differentiation (Fröhling et al., 2005; Roumier et al., 2006; Renneville et al., 2008). The most important transcription factors that have been implicated in the myelomonocytic development are PU-1 for early myeloid commitment, C/EBP for granulocyte maturation, and vitamin D3 (VD) receptor (VDR) and MafB for monocyte-macrophage differentiation (Sieweke and Graf, 1998; Friedman, 2002; Mueller et al., 2002; Gemelli et al., 2008).

The potential of the currently available cytotoxic chemotherapies to treat AML might have reached its limit (Löwenberg et al., 1999; Ravandi et al., 2007). Moreover, the majority of patients with AML are 60 yr of age or older and, in this population, high-dose chemotherapy is associated with a high rate of morbidity and mortality. Although results of new therapeutic strategies have improved steadily in younger adults over the last 20 yr, there have been fewer improvements in outcome among elderly patients (Löwenberg et al., 2009). Based on the emerging knowledge of the biology of AML, new targeted therapeutic approaches need to be developed to interrupt proliferation, induce apoptosis, and/or override the differentiation block.

The current treatment modality for the induction of a terminal differentiation program in AML has only been achieved in acute promyelocytic leukemia (APL or AML3) by the use of differentiating agents combined with chemotherapy (Chen et al., 1994; Zhu et al., 2001; Wang and Chen, 2008). In most of the cases, APLs are characterized by the translocation t(15;17), which encodes a fusion of the promyelocytic leukemia and retinoic acid receptor α proteins. The use of all-trans retinoic acid (ATRA) with chemotherapy was a major breakthrough in APL therapy. It has dramatically improved the prognosis from poor to a high cure rate (~90% of patients; Wang and Chen, 2008). The use of arsenic trioxide (ATO) since the early 1990s further improved the clinical outcome of refractory or relapsed as well as newly diagnosed APL (Wang and Chen, 2008). Current evidences are now available to show that differentiation is not the only mechanism explaining the therapeutic efficacy of ATRA or ATO in clearing APL, as retinoic acid also triggers growth arrest of leukemia initiating cells (Nasr et al., 2008).

Like ATRA, VD belongs to the steroid superfamily and plays a critical role in regulating numerous cellular and physiological responses. VD associates with its cognate receptor (VDR) to form a heterodimer with the retinoid X receptor. This complex then binds to the VD responsive element, which is present in the promoter region of target genes, thereby inducing changes in gene transcription (Hughes et al., 2009). VD also activates a variety of protein kinases, such as the three families of mitogen-activated protein kinase (MAPK; ERK, JNK, and p38), protein kinase C, or Src family kinases by alternative signaling pathways which are not fully characterized (Wang et al., 2003). The active metabolite of VD, $1\alpha,25(OH)_2D_3$, which is known as calcitriol, has antiproliferative effects, can activate apoptotic pathways, and can inhibit angiogenesis (Deeb et al., 2007). In the hematopoietic system, numerous studies on AML blasts, leukemic cell lines, and primary myeloid precursors showed that VD induces cell differentiation into monocytes (Abe et al., 1981; Koeffler et al., 1984; Hmama et al., 1999; Bastie et al., 2004; Ji and Studzinski, 2004; Gemelli et al., 2008; Hughes et al., 2009). Encouraging clinical trials have suggested that VD could be effective as a differentiating agent in the treatment of AML and myelodysplastic syndrome (MDS), but hypercalcemia has limited its use (Ferrero et al., 2004; Srivastava and Ambrus, 2004; Deeb et al., 2007).

Iron (Fe) is required as a cofactor for several critical cellular enzymes involved in energy metabolism and cell proliferation and is therefore essential for all living cells. Iron exists in two oxidation states, the ferrous (Fe^{2+}) and the ferric (Fe^{3+}) forms, which participate to the generation of reactive oxygen species (ROS) through the Fenton reaction. In this process, free cytosolic iron generates hydroxide anions and hydroxyl radicals from hydrogen peroxide ($Fe^{2+} + H_20_2 \leftrightarrow Fe^{3+} + OH^- + OH^{\bullet}$; Fenton et al., 1964) which can lead to cellular damages (Davies, 2005). Therefore, iron chelators have been proposed to be anti-oxidant agents (Kalyanaraman, 2007). However, iron chelators have also been shown to induce the generation of ROS under specific conditions (Chaston et al., 2004).

The transferrin receptor (CD71/TfR1) is an evolutionarily conserved receptor that is essential for the uptake of iron in mammalian cells (Trowbridge and Shackelford, 1986;

different iron deprivation treatments, in contrast to many genes (1,094) that are altered by the iron chelators DFO and DFX. Genes with an intensity >50 and a p-value <0.001 were considered relevant. (b) Fold change variations of gene expression in differentiated cells relative to untreated cells. A24 and the iron chelators up-regulated monocyte/macrophage-specific genes and down-regulated myelocyte-specific genes. Up-regulation is represented on the positive scale, and down-regulation is indicated on the negative scale. (c) Fold increase of CD14 and CD11b expression after flow cytometry (mean fluorescence intensity [MFI] relative to untreated cells) in HL60 cell line treated with 10 µg/ml A24, 5 µM DFO, or 3 µM DFX for 72 h (mean ± SEM, $n = 3$). (d) Fold increase of CD14 and CD11b expression evaluated by flow cytometry (MFI relative to untreated cells) in U937 (white), THP1 (dark gray), OCI-AML3 (black), and NB4 (light gray) cell lines treated with 10 µg/ml A24, 5 µM DFO, or 3 µM DFX for 72 h (mean ± SEM, $n = 3$). (e) MGG-stained cytospins of HL60 cells treated with 250 nM VD, 10 µg/ml A24, 5 µM DFO, or 3 µM DFX for 72 h. The control cells show an immature myeloblastic phenotype: a high nucleus-to-cytoplasm ratio, a hyperbasophilic cytoplasm, and numerous azurophilic granules. The A24- or iron chelator–treated cells show a decrease in the nucleus-to-cytoplasm ratio, the loss of granules, and cytoplasmic basophilia and irregular cytoplasmic contours, all typical of mature monocytes. Bars, 10 µm. Representative photos of three independent experiments are shown. (f) FACS analysis of CD14 expression in HL60 cells treated with A24 (green line), DFO, and DFX (blue lines) in the presence or absence of 5 µM $FeCl_3$ (gray line) for 72 h. The filled histograms represent staining with the isotype control antibody. One representative experiment of three experiments is shown. *, $P < 0.05$; **, $P < 0.01$; ***, $P < 0.001$.

Lim et al., 1987; Daniels et al., 2006b). Cancer cells overexpress TfR1 and are more sensitive to iron depletion than their normal counterparts, most probably because of their high proliferative capacities (Faulk et al., 1980; Gatter et al., 1983). TfR1 is a validated target for anti-cancer therapy using both mAbs and drug-conjugated transferrin (Trowbridge and Domingo, 1981; Daniels et al., 2006a). We have previously characterized an anti-TfR1 antibody (A24) that exhibits potential activity as a therapeutic anti-cancer agent (Moura et al., 2001). A24 specifically binds to TfR1^{high} cells, competes with iron-loaded transferrin (Fe-Tf) for receptor binding, and impairs receptor recycling, thereby drastically impairing iron uptake (Moura et al., 2004; Lepelletier et al., 2007; Callens et al., 2008). Iron chelators have also been proposed for several years as an alternative anti-cancer therapy and effectively induce cell growth arrest and apoptosis in cancer cells in vitro and in vivo (Richardson et al., 1994, 2009; Le and Richardson, 2004; Whitnall et al., 2006).

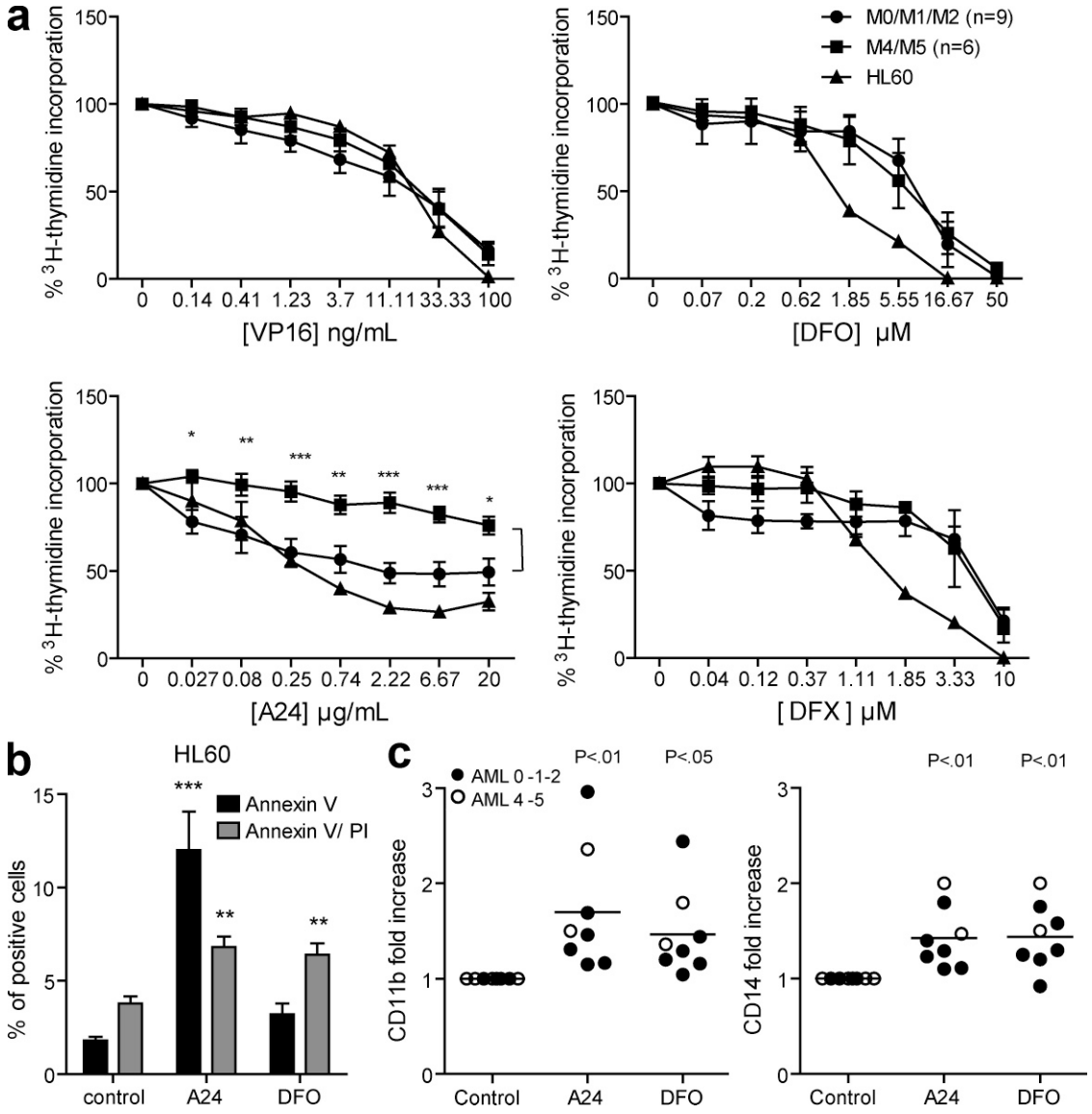

Figure 2. Iron deprivation inhibits proliferation and induces differentiation of AML blasts. (a) Fresh AML blasts or HL60 cells were cultured with increasing concentrations of A24 (0–20 µg/ml), DFO (0–50 µM), DFX (0–10 µM), or VP16 (0–100 ng/ml) for 72 h, followed by a 16-h period of [^{3}H]-thymidine incorporation. Thymidine incorporation (percentage over the control) was plotted as the mean ± SEM of grouped M0/M1/M2 (n = 6) or M4/M5 (n = 9) subtypes patients. Cell proliferation for each patient was measured in triplicate. (b) HL60 cells were cultured in the presence or absence of 10 µg/ml A24 or 5 µM DFO for 72 h. Early and late apoptosis was evaluated by flow cytometry using annexin V–FITC/PI labeling (mean ± SEM, n = 3). *, P < 0.05; **, P < 0.01; ***, P < 0.001. (c) CD14 and CD11b expression in blasts from AML patients treated with A24 and DFO for 72 h. The expression of the differentiation markers was normalized by calculating the fold increase of the MFI relative to the control cells. The filled symbols represent the M0/M1/M2 AML subtypes, and the M4/M5 subtypes are empty symbols. One representative experiment of three is presented for each patient. The mean (horizontal bars) of the eight patients is shown.

The molecular mechanisms underlying the anti-tumor effect of iron-chelating therapeutic approaches still need to be fully elucidated (Napier et al., 2005; Fu and Richardson, 2007). We aimed to characterize these mechanisms and to validate their potential value in AML therapy. In this paper, we show in vivo, in vitro, and ex vivo that targeting iron homeostasis induces blast differentiation toward the monocyte lineage, which is dependent on the modulation of ROS levels and the activation of the MAPK pathway. Importantly, iron deprivation induces VDR gene expression and VDR phosphorylation, providing the rationale for the combination of iron chelation and VD therapies. The synergistic effect of this association amplified the activation of the MAPK–JNK pathway and VDR-targeted genes. Finally, we provide data, in the form of a case report, showing the efficacy of this combination in the induction of tumor cell differentiation in an AML patient. This study provides the proof of concept for the use of combination of iron chelators and VD in AML therapy.

RESULTS

Targeting of iron homeostasis induces AML cell differentiation

To gain new insights in the molecular mechanisms involved in the anti-tumor activity of iron-chelating therapeutic approaches, we sought to identify genes that are affected both by iron chelators (deferoxamine [DFO] and deferasirox [DFX]) and by impairment of Fe-Tf uptake (using the anti-TfR1 mAb A24 [Moura et al., 2004; Lepelletier et al., 2007; Callens et al., 2008]). Indeed, A24 targets TfR1 (the major receptor involved in the iron entry in the cells), whereas iron chelators can also capture other bivalent ions (e.g. Mn^{2+}, Cu^{2+}, or Zn^{2+}) which could modulate genes irrelevant to iron homeostasis. Thus, identification of overlapping genes allows us to avoid selecting off-target genes. We focused our first studies in a cell line (HL60) to avoid heterogeneity in the data related to the multiple genetic events that have been implicated in AML oncogenesis. An analysis of the collected data revealed that 105 genes were similarly modulated by the three iron deprivation agents (Fig. 1 a and Table S1). Among these genes, several were related to cell differentiation. Markers of monocytes or activated macrophages were up-regulated, whereas granulocyte markers were down-regulated (Fig. 1 b). These results were confirmed by real-time quantitative PCR and extended to other AML cell lines from different AML subtypes (Fig. S1 a).

We further tested the ability of iron deprivation to override the block of cell differentiation observed in AML cells. We followed the expression of CD14 and CD11b monocyte cell surface markers (Kansas et al., 1990) after iron deprivation induced by treatment with A24, DFO, or DFX. Expression of both markers was induced by iron deprivation, suggesting that cells underwent differentiation (Fig. 1 c) similar to VD-treated cells (Fig. S1 b). Up-regulation of monocyte cell surface markers, initially detected in myeloblastic cells (HL60), was also observed in cell lines from myelo/monoblastic (OCI AML-3), monoblastic (U937 and THP1), and promyelocytic (NB4) origin (Fig. 1 d).

Induction of cell surface markers in treated cells was accompanied by the characteristic cytological modifications of monocytes, i.e., cytoplasm enlargement and loss of both cytoplasmic basophilia and azurophilic granules (Fig. 1 e and Fig. S1 c). Moreover, HL60 differentiated cells acquired functional properties of monocytes such as esterase activity (Fig. S1 d).

Supplementation of cultures with an excess of soluble iron abrogated expression of differentiation markers induced by iron deprivation (Fig. 1 f) but not by ATRA and VD (Fig. S2), confirming the role of iron availability in AML cell differentiation. We next investigated whether primary cells from AML patients could also be sensitive to iron deprivation therapy. Fresh AML blasts from different AML subtypes (categorized according to the French-American-British [FAB] classification system [Bennett et al., 1976]) were isolated at the time of diagnosis (Table S2, complete list of AML subtypes and biological parameters for the patients used in this study) and were cultured in the presence of A24 and DFO. An arrest of cell proliferation (Fig. 2 a) and induction of apoptosis (Fig. 2 b) were observed concomitantly to CD14 and CD11b expression (Fig. 2 c), indicating that, similar to cell lines, blasts from different AML subtypes, even if heterogeneous in the oncogenic events leading to their arrest in differentiation (Löwenberg et al., 1999), are susceptible to differentiation therapy based on iron deprivation.

Targeting of iron homeostasis induces primary progenitor differentiation toward the monocyte lineage

To verify if iron homeostasis plays a role in the differentiation of primary granulocytes and monocytes, we tested the effect of iron deprivation on hematopoietic cord blood progenitors. Iron deprivation agents did not change the total number of colonies derived from $CD34^+$ cells in methylcellulose plates (unpublished data). However, treatment with the iron chelators resulted in an increased number of bipotent CFU-GM colonies (Fig. 3 a) and enhanced the ratio of CFU-M to the detriment of CFU-G colonies (Fig. 3 b), suggesting that chelating iron from hematopoietic precursors induces commitment toward the monocyte over the granulocyte lineage. As expected, because iron is necessary for hemoglobin synthesis (Adamson, 1994) the number of CFU-E colonies was reduced by all the iron deprivation agents (Fig. 3 c).

When differentiation of $CD34^+$ cord blood progenitors into granulocytes was induced in liquid cultures (Fig. S3), >65% of cells were polymorphonuclear cells after 18 d. We therefore added A24 or iron chelators to these granulocyte-oriented cell cultures every 3 d, at concentrations which did not induce cell toxicity (unpublished data). Under these conditions, iron deprivation did not affect cord blood cell proliferation (Fig. 3 d) but rather enhanced their commitment toward the monocyte lineage because there was a consistent up-regulation of genes coding for transcription factors specific for the monocyte lineage, such as

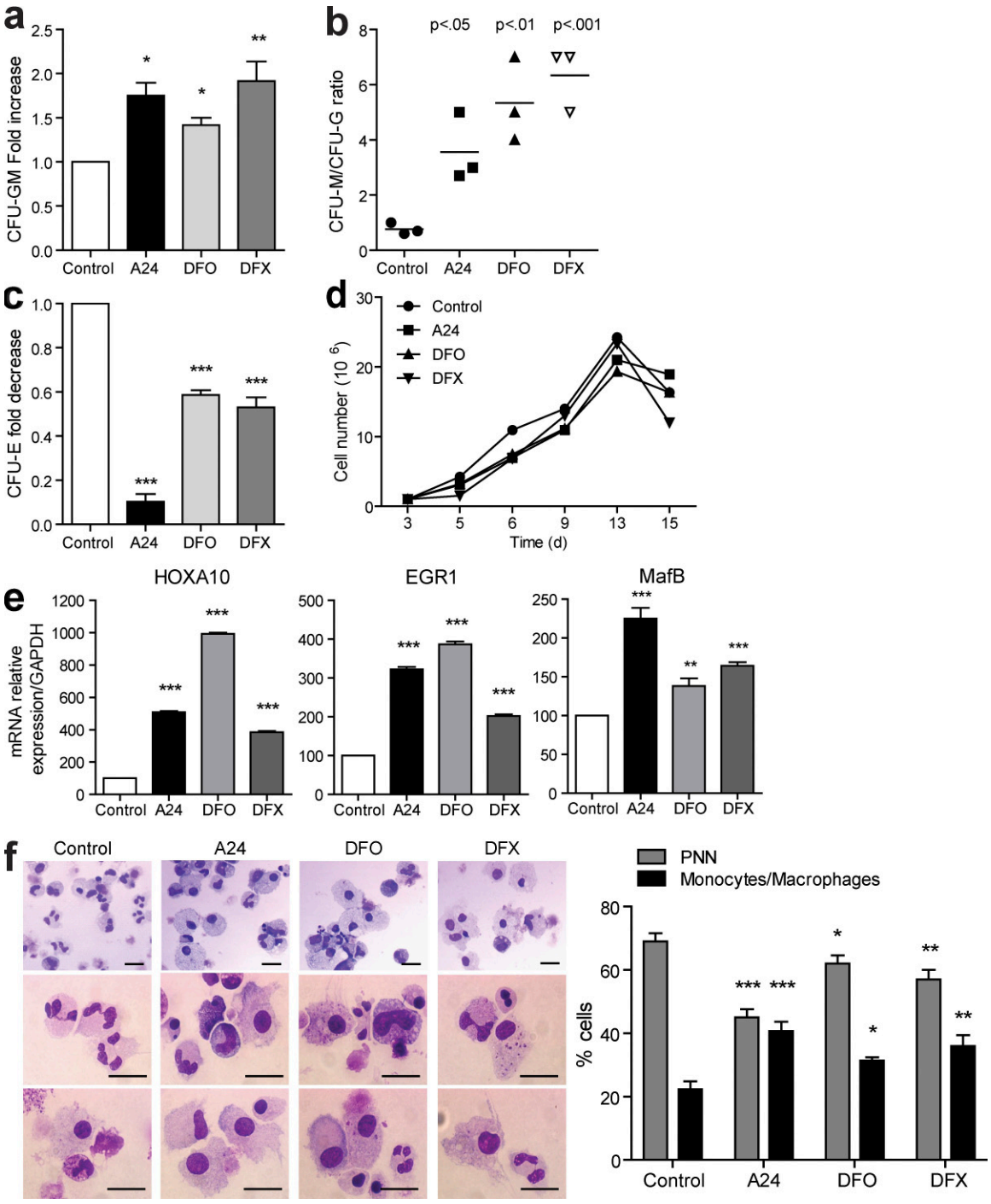

Figure 3. Iron deprivation induces the differentiation of primary progenitors into monocytes. CD34+ cord blood progenitors were plated in methylcellulose containing a cocktail of cytokines (Epo, SCF, IL-3, G-CSF, and GM-CSF) in the presence or absence of 10 µg/ml A24, 5 µM DFO, or 3 µM DFX. After 14 d, colonies of each lineage were counted (mean ± SEM, $n = 3$). (a and b) Variations of colonies are represented as the fold increase of CFU-GM (a) or the ratio of CFU-M/CFU-G (b). (c) Fold decrease of CFU-E. (d) Cell numbers and viability measured by Trypan blue dye exclusion during culture. One representative experiment of three is shown. All counts were performed in triplicates. (e) After 48 h of culture, the mRNA expression of *HOXA10*, *EGR1*, and *MAFB* was quantified by quantitative RT-PCR and normalized to the expression of *GAPDH* (mean ± SEM, $n = 3$). (f) Representative photos taken at the end of culture (day 18) are shown. Polymorphonuclear neutrophils are present in the majority of the control cultures, whereas monocytes and macrophages are predominantly present under iron deprivation conditions. The histograms represent the percentage of each leukocyte population from MGG-colored cytospins at day 18 (mean ± SEM, three independent counts of 100 cells each). Bars, 10 µm. *, $P < 0.05$; **, $P < 0.01$; ***, $P < 0.001$.

HOXA10, *EGR1*, and *MafB* (Sieweke et al., 1996; Kelly and Gilliland, 2002; Taghon et al., 2002; Friedman, 2007; Fig. 3 e). Cytological examination confirmed that the monocyte cell number was higher in iron-poor cultures (Fig. 3 f). Therefore, in hematopoiesis, iron availability could be an important factor in determining whether a hematopoietic progenitor cell differentiates toward a monocyte or a granulocyte.

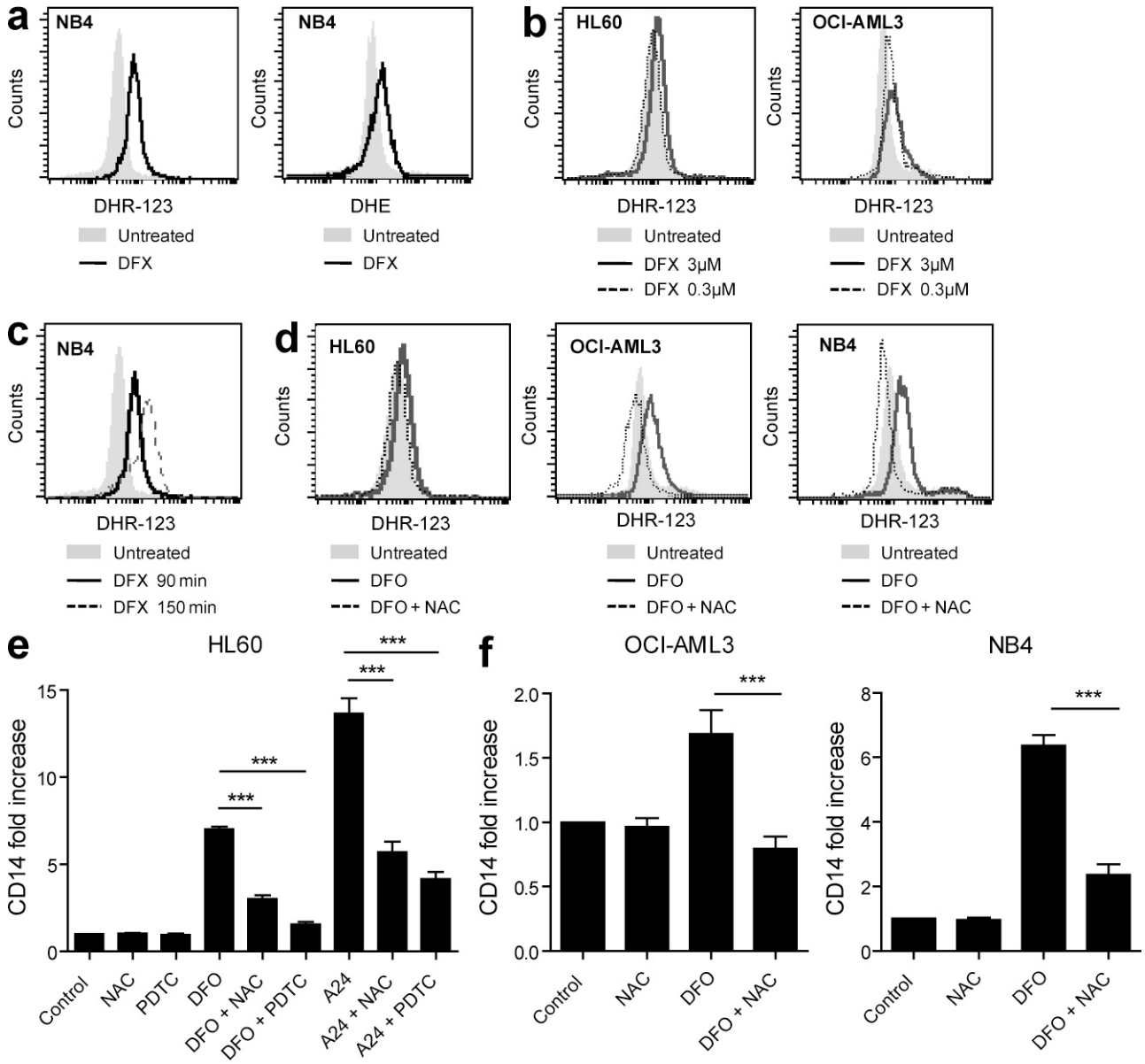

Figure 4. Modulation of ROS levels controls monocyte differentiation in AML cells. (a) Representative flow cytometry analysis showing ROS production by NB4 cells. Cells were stained for 30 min at 37°C with 0.5 µM DHR123 or 1 µM DHE and further treated with 3 µM DFX (continuous line) or not (filled histograms) for 90 min. One representative experiment of three is presented. (b) ROS production in AML cell lines (HL60 and OCI-AML3 cells) is dose dependent. Cells were labeled with DHR123 (as described in a) and treated with 3 µM DFX (continuous line) or 0.3 µM DFX (dashed line) for 90 min or not (filled histograms). One representative experiment of three is presented. (c) Time-dependent production of ROS. NB4 cells were treated with 3 µM DFX for 90 min (continuous line) or 150 min (dashed line). ROS production was evaluated by flow cytometry. One representative experiment of three is presented. (d) Representative flow cytometry data showing specificity of the ROS production by NB4 cells. Cells were stained for 30 min at 37°C with 0.5 µM DHR123 and further treated with 3 µM DFO. Abrogated ROS detection is shown in cell cultures where DFO was added in the presence of the anti-oxidant NAC (dashed line) as compared with control untreated cells (filled histogram). One representative experiment of three is presented. (e) CD14 expression (fold change) in HL60 cells treated with 10 µg/ml A24 and 5 µM DFO in the presence or absence of the anti-oxidant agents (NAC and PDTC) for 72 h (mean ± SEM, $n = 3$). (f) CD14 expression in OCI-AML3 and NB4 cells treated with DFO in the presence or in the absence of the anti-oxidant agent NAC for 72 h (mean ± SEM, $n = 3$). ***, $P < 0.001$.

Iron deprivation–induced cell differentiation is dependent on the modulation of ROS levels

ROS production is highly dependent on the intracellular labile iron pool (LIP). Therefore, to investigate whether iron-chelating agents modulate ROS levels in AML cells, we used a metallo-sensor fluorescent probe (calcein) for LIP measurements (Espósito et al., 2002) and dihydrorhodamine 123 (DHR123) as an indicator of the degree of general oxidative stress or dihydroethidium (DHE) to monitor cellular superoxide production (Owusu-Ansah et al., 2008). As expected, previous addition of iron deprivation agents decreased LIP levels in AML cells and DFX was the fastest and most efficient compound (Fig. S4, a–c). Iron deprivation of cells by DFX (the most permeant chelators) was readily accompanied by ROS formation (Fig. 4 a), which was found to be concentration (Fig. 4 b) and time (Fig. 4 c) dependent. We further confirmed the specificity of ROS detection by preincubating iron-deprived cells with the anti-oxidant *N*-acetyl-L-cysteine (NAC; Fig. 4 d).

Iron chelators had opposite effects depending on whether AML cells were treated during short (1–3 h; Fig. 4, a–d) or long (16–18 h; Fig. S4, d–f) periods of time. In addition, in HL60-cultured cells treated for 16–18 h with iron chelators, the H_2O_2-mediated generation of ROS was abrogated in a dose-dependent manner (Fig. S4, d and e), whereas ATO induced a sustained production of ROS in NB4 cells (Fig. S4 f).

To further clarify which of the pro- or anti-oxidant effects of iron chelators was implicated in monocyte differentiation, iron-deprived AML cells were treated with or without the anti-oxidants NAC or pyrrolidine dithiocarbamate (PDTC). Anti-oxidant prevented the increase in CD14 mediated by iron deprivation differentiation, suggesting that cell differentiation is dependent on the increased ROS levels induced during the early course of cellular iron deprivation (Fig. 4, e and f). Thus, iron-depriving agents control cell differentiation through modulation of ROS levels.

Cell differentiation induced by iron deprivation is dependent on the activation of the MAPK pathway

MAPKs are serine/threonine protein kinases crucial to several biological responses including stress responses to ROS (Whitmarsh and Davis, 1999). The addition of the specific inhibitors of ERK, JNK, and p38 MAPK signaling pathways (which characterize the three MAPK families) abrogated cell differentiation induced by iron deprivation agents (Fig. 5 a). The iron-chelating agents induced the phosphorylation of ERK, p38, and JNK (Fig. 5 b). However, only inhibitors of JNK and p38, but not of ERK, prevented iron deprivation–induced apoptosis (Fig. 5 c).

Iron deprivation–induced cell differentiation shares high similarity with that induced by VD

VD can induce monocyte/macrophage differentiation of both primary cells and myeloid leukemia cell lines (Abe et al., 1981; Koeffler et al., 1984; Hmama et al., 1999; Bastie et al., 2004; Ji and Studzinski, 2004; Gemelli et al., 2008; Hughes et al., 2009). By comparing the pattern of genes induced by VD and by iron-chelating agents in a nonsupervised transcriptome analysis, we found a high similarity between the differentially expressed genes; of the 105 genes that were modulated by iron deprivation, 30 were also modulated by treatment with VD (Fig. 6 a and Table S3). Both VD and the iron-chelating agents up-regulated monocyte markers and down-regulated neutrophil markers (Fig. 6 b). Moreover, in gene chips (Fig. 6 c) and real-time quantitative PCR (Fig. 6 d) analysis, transcription of the *c-Jun* gene was induced by both VD and iron deprivation. Transcripts coding for *c-Fos* were also up-regulated by both treatments (Fig. 6 d), suggesting the involvement of the JNK pathway. Similar results were observed in cell lines from different AML subtypes (Fig. 6 e). To further address the role of JNK, cells were transfected with micro RNA (miRNA) constructs specific for different members of the JNK pathway (namely JNK1, JNK2, and c-Jun; Fig. S5, a–c). miRNA–mediated silencing of c-Jun, JNK1, and JNK2 markedly abrogated cell differentiation induced by iron deprivation agents (Fig. 6 f). Overexpression of each one of the two JNK proteins revealed that JNK1 was the most effective to induce cell differentiation of AML cells (Fig. 6 g).

Given the high similarities shared between VD and iron deprivation agents to induce cell differentiation, we investigated whether iron deprivation of cells could induce VDR signaling (Wang et al., 2003; Himes et al., 2006). As observed for its cognate ligand VD, VDR expression was induced in cells treated by iron-chelating agents (Fig. 6 h). The addition of iron chelators to cells starved of growth factors readily induced the VDR phosphorylation (Fig. 6 i) involved in the control of VDR activity (Jurutka et al., 1996). Altogether, these results indicate that iron-chelating agents are able to induce cell differentiation through the activation of JNK pathway. Iron deprivation also potentiates VDR signaling pathway through VDR expression and VDR phosphorylation.

VD synergizes with iron deprivation agents through the activation of the Jun pathway to induce cellular differentiation

Treatment of cells with both iron chelators and VD drastically increased the up-regulation of monocyte markers CD11b and CD14 (Fig. 7 a). We consequently investigated whether the combination of iron-chelating agents (as the iron chelator DFO and the anti-TfR1 A24) and VD had a synergistic effect. Applying the combination index (CI) isobologram method (Chou and Talalay, 1984), we evaluated interactions between DFO and VD, or A24 and VD (Figs. S6, a–d). At the concentration inducing 50% of $CD14^+$ cells, CI values for the combination of DFO and VD, or A24 and VD, were <1 (0.87 and 0.89, respectively), indicating a synergistic interaction. Both combinations were accompanied by morphological changes in the treated cells (Fig. 7 b) and by higher expression of VDR (Fig. 7 c). The physiological relevance of increased VDR gene expression was demonstrated by the robust increase in the transcription of its

downstream target genes, cathelicidin (1,000-fold increase) and CYP24A (6,000-fold increase; Fig. 7 d), and *c-Fos* and *c-Jun* (Fig. 7 e). Moreover, the phosphorylation of JNK increased in response to treatment with both VD and iron deprivation (Fig. 7 f). The combined effect of VD and iron chelators was specific to VDR signaling because iron chelators did not potentiate the ability of ATRA to promote cell differentiation in HL60 cells (Fig. S7). Finally, the efficacy of the combined therapy was validated ex vivo in primary cells from AML patients (Fig. 7 g).

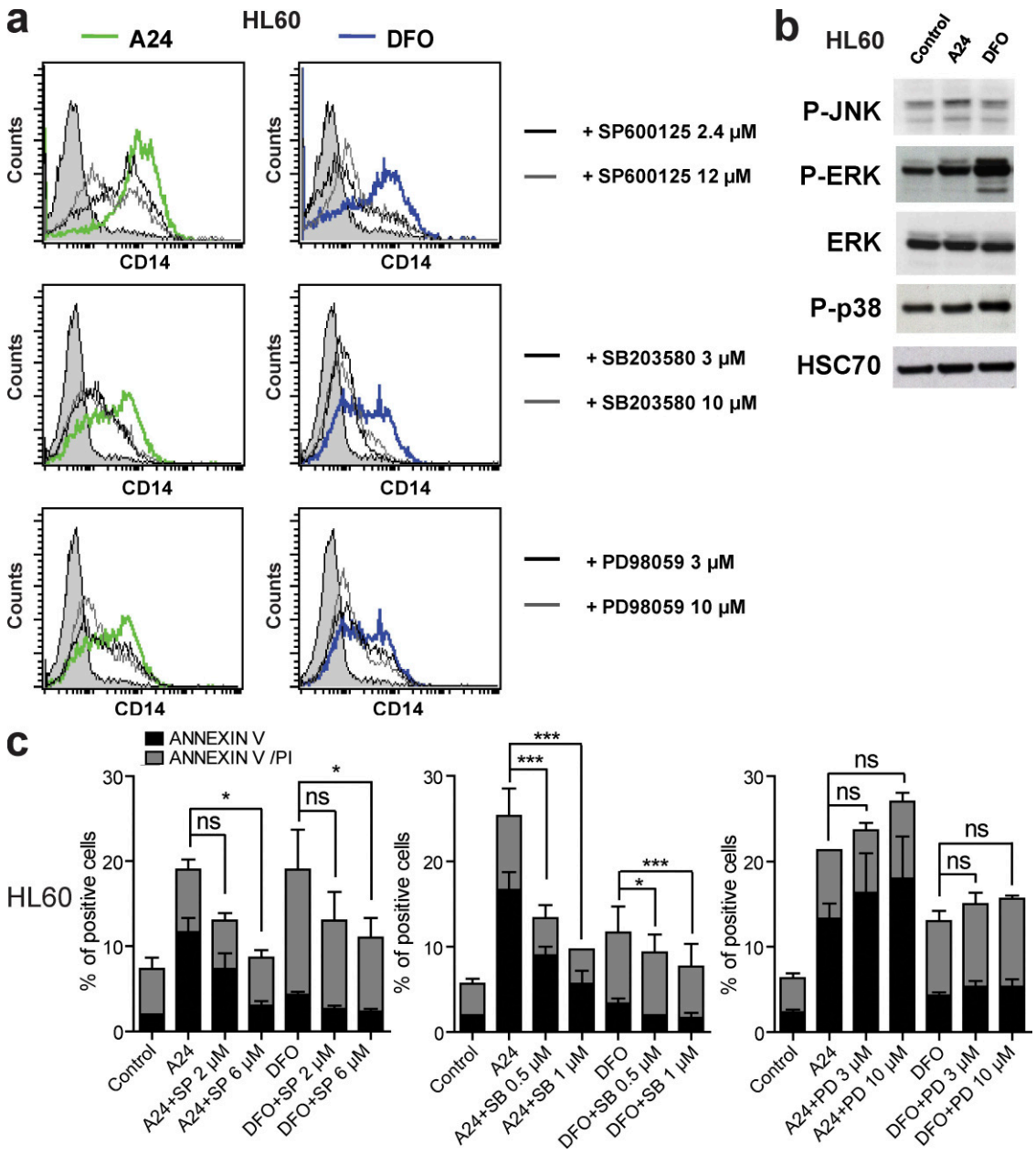

Figure 5. Cell differentiation and apoptosis are controlled by MAPK activation. (a) CD14 expression on HL60 cells cultured in the presence or absence of A24 (green) or DFO (blue) and treated with a JNK inhibitor (SP600125) at 2.4 or 12 µM, with a p38 inhibitor (SB203580) or an ERK inhibitor (PD98059) at 3 or 10 µM, or mock treated for 72 h. Filled histograms represent staining with the isotype control antibody. One representative experiment of three experiments is shown. (b) Serum-starved HL60 cells were incubated with 10 µg/ml A24 or 3 µM DFO for 30 min at 37°C. Whole cell extracts were analyzed by immunoblotting, demonstrating the phosphorylation of JNK (p-JNK), ERK (p-ERK), and p38 (p-p38). One representative experiment of three experiments is shown. HSC70 and ERK were used as equal loading controls. (c) Histograms representing early and late apoptosis/necrosis using flow cytometry with annexin V–FITC/PI labeling. HL60 cells were cultured for 72 h in the presence or absence of 10 µg/ml A24 or 5 µM DFO and treated with 2 or 6 µM JNK inhibitor (SP600125 [SP]), 0.5 or 1 µM p38 inhibitor (SB203580 [SB]), 3 or 10 µM ERK inhibitor (PD98059 [PD]), or mock treated (mean ± SEM, $n = 3$). *, $P < 0.05$; ***, $P < 0.001$.

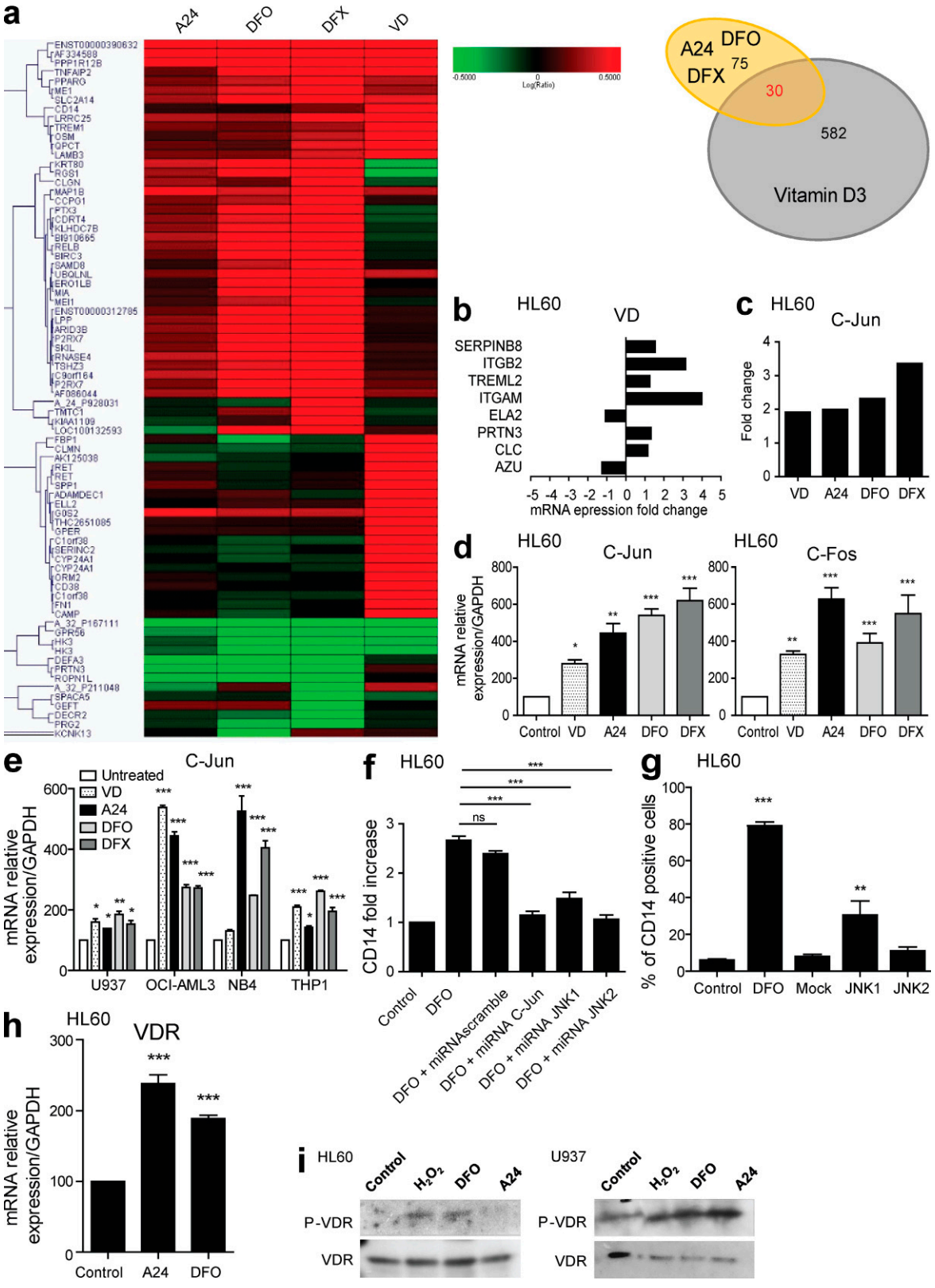

Figure 6. Cellular differentiation induced by iron deprivation is dependent on the activation of the JNK and VDR signaling pathways.
(a) Hierarchical gene clustering by unsupervised microarray analysis in HL60 cells treated with 250 nM VD or iron chelating agents (A24, 10 µg/ml; DFO, 5 µM or DFX, 3 µM). Only genes with a fold change >4 and a p-value $<10^{-15}$ are shown (left). A Venn diagram is shown, demonstrating that among the 105 genes that were specifically induced by iron deprivation, 30 were modified by treatment with VD (right). (b) Histograms representing the variation of

In vivo efficacy of combined iron homeostasis and VD treatment through the activation of the MAPK–JNK pathway

Based on these observations, we postulated that the combination of iron deprivation and VD could intensify their antileukemic properties. Therefore, the efficacy of differentiation therapy was further evaluated in vivo in a mouse tumor xenograft model. A single dose of A24 completely inhibited the growth of HL60 transplanted tumors, whereas treatment with DFO increased survival and decreased the tumor size (Fig. 8, a and b). Using this model, we did not observe a significant reduction in tumor growth for mice treated with VD alone (Fig. 8 c). However, the combination of VD with DFO significantly reduced tumor growth (Fig. 8 d). The parameters of serum iron homeostasis, such as serum transferrin and ferritin levels, were significantly modified in the treated mice, which is an indication of effective iron deprivation (Fig. 8 e). The reduced tumor growth was associated with tumor cell apoptosis, which are features of cellular differentiation and MAPK phosphorylation (ERK and JNK; Fig. 8 f). In mice xenografted with OCI-AML3 cells, DFO greatly improved event-free survival (Fig. S8 a). There was no significant difference in event-free survival between mice treated with DFO and DFO + VD. However, a significant reduction in tumor growth was observed only in mice that received the DFO + VD association, although the DFO-treated mice presented reduction in tumor growth compared with control which did not reach significance (Fig. S8 b).

Case report

Because both iron chelators and VD analogues are safe drugs currently used as therapies in the treatment of diseases other than leukemia, their effectiveness in one AML patient was evaluated. A 69-yr-old man had a recent transformation of MDS into AML. After high-dose chemotherapy, the patient remained in non-blastic aplasia. 7 mo after the diagnosis, blasts reappeared in the blood. High-dose chemotherapy was denied, and treatment with an iron chelator (1 g/d DFX) and 25-hydroxycholecalciferol (4,000 IU/d) was initiated.

Blast counts, although progressing before therapy, were decreased upon iron chelation and vitamin D therapy, and pancytopenia was partially reversed, accompanied by an increase in monocyte numbers (Fig. 9 a) without inducing hypercalcemia (Fig. 9 b). Importantly, May Grünwald Giemsa (MGG) blood smears revealed an increased number of differentiating cells toward the monocyte lineage, suggesting that they were derived from the blast pool (Fig. 9 c). Cell sorting (Fig. 9 d), followed by fluorescent in situ hybridization analysis, showed that the original trisomy 8 found in the blasts of the patient (Fig. 9 e) was segregated with the sorted mature monocyte population but not with lymphocytes or NK cells (Fig. 9 f), confirming that the circulating monocytes were derived from the blast pool. In addition, the patient's quality of life was improved because red cell and platelet transfusion needs were decreased. Furthermore, the patient could control several microbial infections that otherwise would have been life threatening, suggesting that the patient's immune status was partially restored. These data underscore the differentiating efficiency of combined therapy in human AML.

DISCUSSION

We show in this paper that iron homeostasis plays a key role in the control of myeloid differentiation in both normal and pathological situations. Iron deprivation of undifferentiated myeloid cells, either through iron chelation or through blocking of iron uptake, induced transcription of several markers of the monocyte/macrophage lineage. At the same time, iron deprivation shunted progenitors away from the granulocytic lineage by dampening the transcription of granulocyte-specific markers. Morphological, phenotypic, and functional analyses confirmed and extended these observations. Not only did iron deprivation induce primary progenitor commitment toward the monocyte lineage, it also reestablished differentiation in AML blasts/cell lines.

Recent cumulated data in the literature have shown that ROS can modulate the activation of signal transduction pathways involved in several cellular functions such as cell proliferation and differentiation (Sattler et al., 1999). Specifically, in the mammalian hematopoietic system, it has been recently reported that hematopoietic stem cells produce low levels of ROS, which are increased in common myeloid progenitors. Modulation in ROS levels seems to be important in the control of myeloid precursor differentiation (Tothova et al., 2007).

expression (fold change relative to untreated cells) of genes found in mature monocytes (up-regulated) or neutrophils (down-regulated) that were previously modified by A24 and the iron chelators. These genes are similarly regulated by VD treatment. Up-regulation of gene transcription is represented on the positive scale, and down-regulation is shown on the negative scale. (c) Genechip fold change in *c-Jun* expression after treatment with VD or iron deprivation. (d) *c-Fos* and *c-Jun* mRNA levels evaluated by quantitative RT-PCR and normalized to *GAPDH* mRNA in HL60 cells treated for 48 h with the indicated agents (VD, 250 nM; A24, 10 µg/ml; DFO, 5 µM or DFX, 3 µM; mean ± SEM, $n = 4$). (e) *c-Jun* mRNA level evaluated by quantitative RT-PCR and normalized to *GAPDH* mRNA in U937, OCI-AML3, NB4, and THP1 cell lines treated for 48 h with the indicated agents (VD, 250 nM; A24 10 µg/ml; DFO, 5 µM or DFX, 3 µM; mean ± SEM, $n = 4$). (f) Fold increase of CD14 expression in HL60 cells transfected with the indicated miRNA constructs: scrambled control miRNA, miRNA-C-Jun, miRNA-JNK1, or miRNA-JNK2. 48 h later, each transfected cells were treated with 5 µM DFO to induce cell differentiation. CD14 expression was evaluated by flow cytometry gating on cells on the basis of their GFP expression 72 h after transfection (mean ± SEM, $n = 3$). (g) Percentage of differentiated cells induced in HL60 treated for 72 h with DFO or transfected with JNK1-GFP and JNK2-GFP expression plasmids or mock electroporated. CD14 expression was evaluated 72 h after treatments (mean ± SEM, $n = 3$). (h) *VDR* mRNA level evaluated by quantitative RT-PCR and normalized to *GAPDH* mRNA in HL60 cells treated for 48 h with the indicated agents (A24, 10 µg/ml or DFO, 5 µM; mean ± SEM, $n = 4$). *, $P < 0.05$; **, $P < 0.01$; ***, $P < 0.001$. (i) Serum-starved HL60 and U937 cells were incubated with 0.5 µM H_2O_2, 10 µg/ml A24, or 3 µM DFO for 10 min at 37°C. Phosphorylation of VDR (P-VDR) in whole cell extracts was analyzed by immunoblotting. VDR was used as loading control. One representative experiment of three is shown.

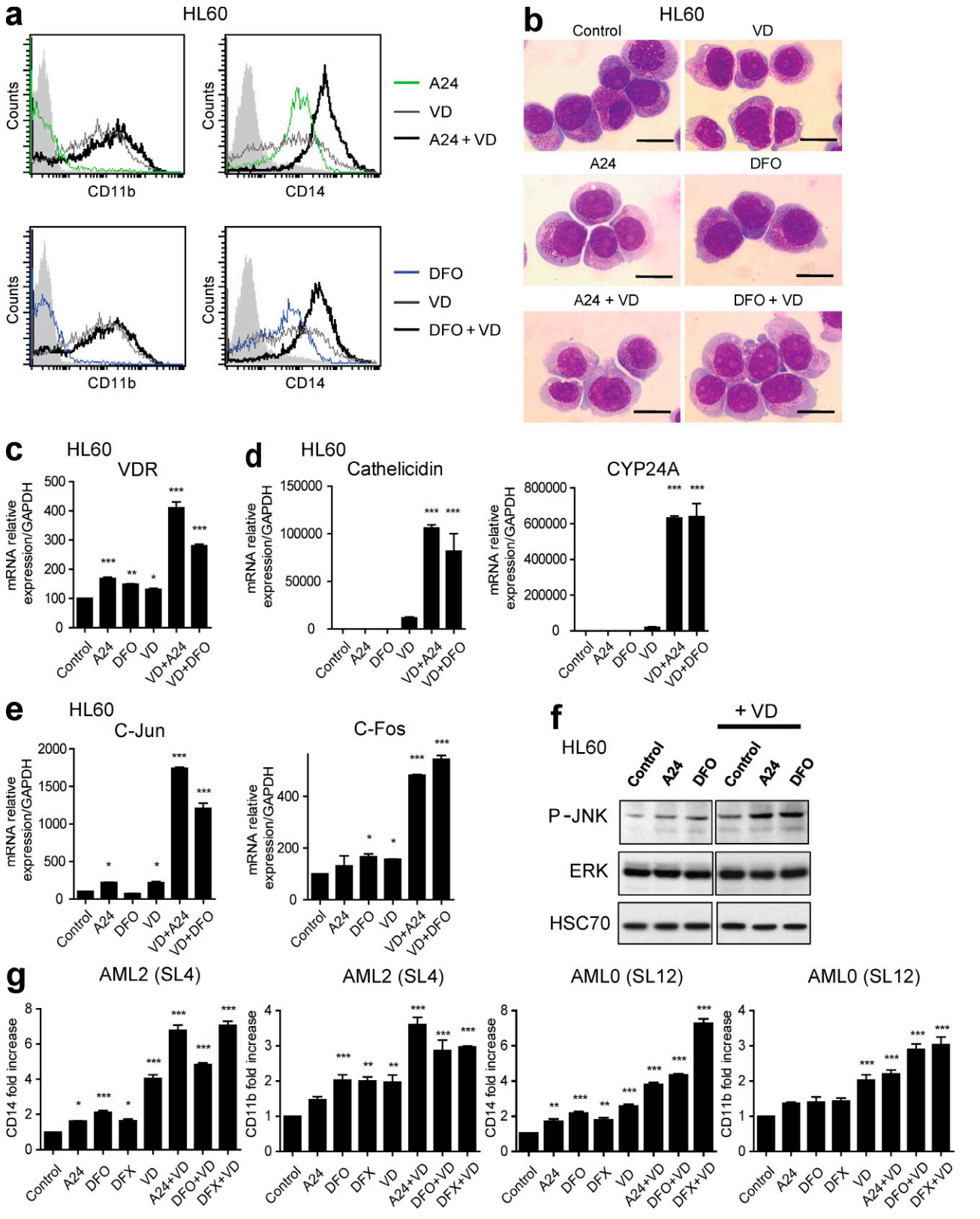

Figure 7. VD synergizes with iron deprivation agents to activate the Jun pathway and induce cellular differentiation. (a) Flow cytometric analysis of CD14 and CD11b expression on HL60 cells treated with 10 µg/ml A24 (green line) or 5 µM DFO (blue line), with 250 nM VD (gray lines) or a combination of VD and iron-chelating agents (black lines) for 72 h. The filled histograms represent staining with the isotype control antibody. One representative experiment of three is shown. (b) HL60 cells were incubated with 10 µg/ml A24 or 3 µM DFO and treated with 250 nM VD or mock treated

This process seems to be conserved throughout evolution because *Drosophila melanogaster* multipotent hematopoietic progenitors display increased levels of ROS which are down-regulated during differentiation (Owusu-Ansah and Banerjee, 2009). However, factors controlling ROS production in myeloid progenitors are not well known. We show in this paper that intracellular LIP could be one of these factors playing a critical role in controlling ROS levels and, thus, cell differentiation in the hematopoietic system.

Scavenging ROS from *Drosophila melanogaster* hematopoietic progenitors delays mature blood cell differentiation, which is dependent on the MAPK JNK (Owusu-Ansah and Banerjee, 2009). In this paper, we show that both genetic and pharmacological inactivation of the MAPK–JNK pathway inhibited iron deprivation-induced cell differentiation. Furthermore, pharmacological blocking of ROS abrogated iron deprivation–induced cell differentiation, suggesting that ROS and MAPK pathways are linked, most probably by the direct effect of ROS on MAPK activation (Martindale and Holbrook, 2002). Signal transduction cascades of MAPK pathways frequently converge to amplify signaling (Johnson and Lapadat, 2002; Lopez-Bergami et al., 2007). Inhibition of ERK and p38 pathways prevented cell differentiation induced by iron deprivation. Blocking of the ERK pathway did not block apoptosis induced by iron chelators, suggesting that redundant and nonredundant MAPK signaling pathways are involved in the control of AML cell differentiation and apoptosis. In agreement, it has been previously shown that the MAPK–ERK pathway is constitutively active in AML cells and in G-CSF–mobilized $CD34^+$ precursors and inhibition of ERK pathway promotes growth arrest rather than apoptosis (Ricciardi et al., 2005). Combining iron chelation therapy with other MAPK/ERK activators, such as G-CSF, remains to be evaluated. Altogether those data suggest that cross talk between MAPK pathways could cooperate to regulate AML cell differentiation and its sensitivity to cytotoxic agents.

In the majority of the experiments presented in this paper, TfR1 targeting by A24 mimicked the effect of iron chelators at least in in vitro and ex vivo settings. Because each of the iron-chelating agents has its own chemical/biochemical characteristics (such as the structure or cell-permeant properties of the different iron chelators and cell targeting specificity of the monoclonal antibody) and pharmacological properties (such as the kinetics and half-life), the intensity of the response varied among them. For example, in tumor xenograft experiments, A24 mAb totally inhibited tumor engraftment, whereas iron chelators delayed the tumor growth, a difference probably involving additional effects of A24 such as antibody-dependent cellular cytotoxicity or complement-dependent cytotoxicity. In addition, A24 could exert a specific target effect by inducing TfR1 down-regulation specifically on TfR^{high} tumor cells (Moura et al., 2004; Lepelletier et al., 2007; Callens et al., 2008), whereas iron chelators are more likely to induce TfR1 messenger RNA (mRNA) stability by posttranscriptional mechanisms.

The principal molecular mechanism drawn from the experiments reported in this paper links the signaling pathways activated by iron deprivation and by VD. Gene expression studies showed a high similarity (30% common genes) between genes modulated by VD and the set of 105 genes targeted by iron deprivation. In addition, iron deprivation induced both VDR gene expression and VDR phosphorylation. The phosphorylation of VDR on serine 208 by casein kinase II has been shown to control activation of VDR gene transcription and VDR target genes expression (Jurutka et al., 1996). Therefore, iron deprivation could induce, by itself, the activation of VDR signaling pathway. Furthermore, the combination of iron deprivation agents and differentiating therapies acted synergistically, increasing AML cell differentiation.

Altogether, our data identified a mechanism involving sequentially iron-deprivation, ROS production, and activation of MAPK pathways, further amplified by induction of VDR expression and phosphorylation, culminating in monocyte/macrophage differentiation. Recent studies showed an unexpected constitutive activation of Syk tyrosine kinase in AML blasts (Hahn et al., 2009). Gefitinib has been identified as a Syk tyrosine kinase inhibitor (Hahn et al., 2009) and reported to be a potent inducer of AML cell differentiation in preclinical settings (Boehrer et al., 2008). These studies unveiled Syk as a previously unsuspected regulator of AML differentiation. Although the molecular pathways regulating the activation of Syk in AML cells remain unknown, a study by Agramonte-Hevia et al. (2003) reported that VD-induced cell differentiation down-regulated the high Syk activation observed in undifferentiated THP-1 cells. Therefore, down-modulation

for 72 h. Cytospins for the treated cells were stained with MGG. Monocyte differentiation is observed with the loss of granulation and basophilia, vacuole appearance, and cytoplasm enlargement. Bars, 10 µM. Representative photos of three independent experiments are shown. (c) The *VDR* mRNA level, evaluated by quantitative RT-PCR and normalized to *GAPDH* in HL60 cells treated for 6 h with the indicated agents (A24, 10 µg/ml; DFO, 5 µM; or VD, 250 nM; mean ± SEM, $n = 4$). (d) The mRNA level of *Cathelicidin* and *CYP24A*, evaluated by quantitative RT-PCR and normalized to *GAPDH*, in HL60 cells treated for 6 h with the indicated agents (A24, 10 µg/ml; DFO, 5 µM; or VD, 250 nM; mean ± SEM, $n = 4$). (e) The mRNA level of *c-Fos* and *c-Jun* genes, evaluated by quantitative RT-PCR and normalized to *GAPDH*, in HL60 cells treated for 16 h with A24, DFO, and VD as described in c (mean ± SEM, $n = 4$). (f) Serum-starved HL60 cells were incubated with 10 µg/ml A24 or 3 µM DFO and treated with 250 nM VD or mock treated for 30 min at 37°C. Whole cell extracts from the treated cells were analyzed by immunoblotting, demonstrating the increased phosphorylation of JNK when VD is combined with A24 or DFO. HSC70 and total ERK were used as loading controls. One representative experiment of three is shown. (g) Fold increase of CD14 and CD11b expression analyzed by flow cytometry (MFI relative to untreated cells) in primary blasts from two AML patients, identified as SL4 (AML2 FAB subtype) and SL12 (AML0 FAB subtype). Cells were treated with 10 µg/ml A24, 5 µM DFO, 3 µM DFX, or 250 nM VD or their association as indicated for 72 h (mean ± SEM, $n = 3$). *, $P < 0.05$; **, $P < 0.01$; ***, $P < 0.001$.

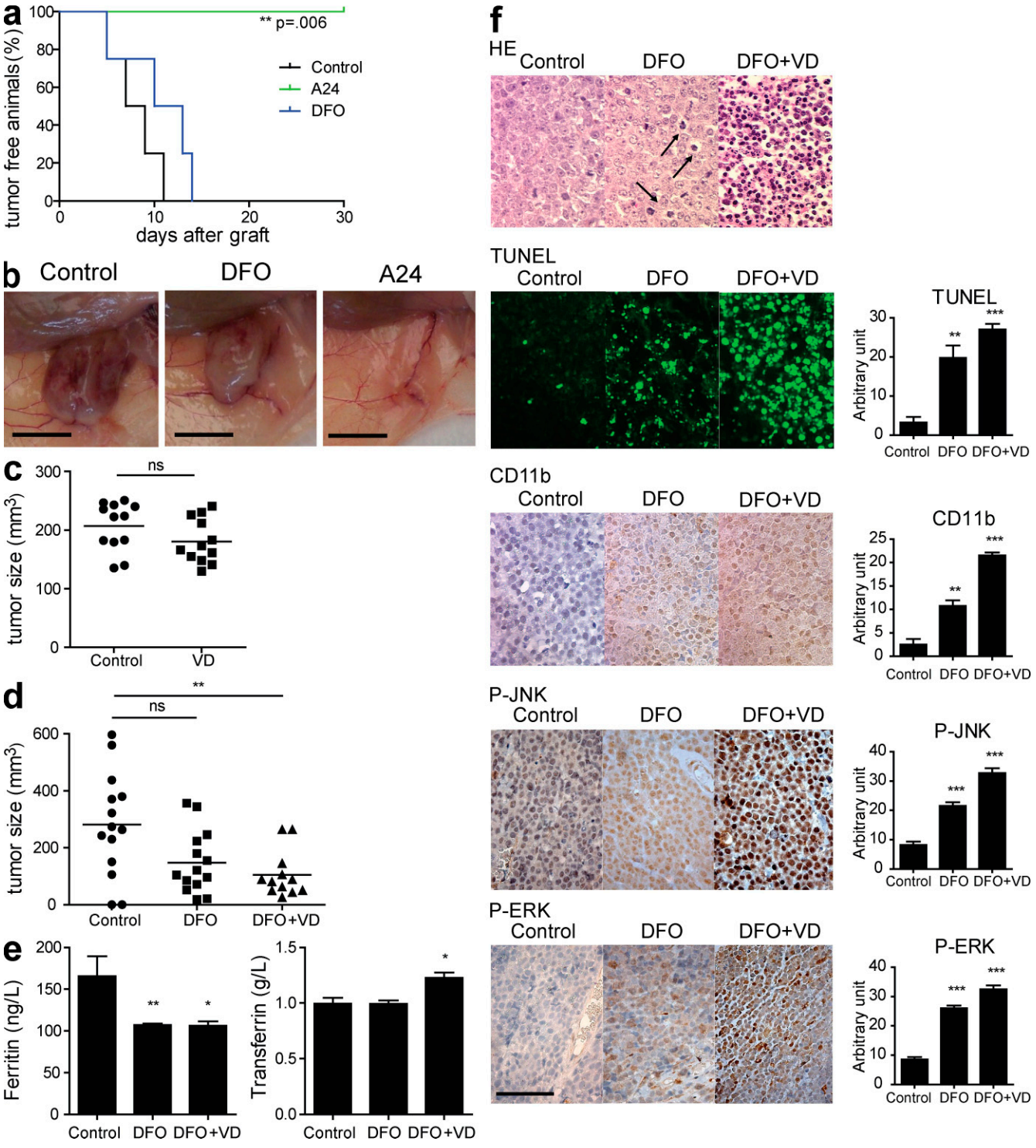

Figure 8. Anti-tumor effect of iron deprivation combined with VD in Nude mice. (a) Kaplan-Meier plot of the percentage of tumor-free mice among mice treated with vehicle (control), A24 (single intravenous dose of 40 mg/kg), and DFO (20 mg 5×/wk) after subcutaneous xenograft with HL60 cells ($n = 4$ in each group). The p-value was determined using the log-rank test. One representative experiment of three is shown. (b) Representative photographs of xenografted tumors from Fig. 5 a. Bars, 10 mm. (c) Tumor size (measured at day 25) in HL60 cells xenografted in Nude mice. Individual tumor sizes are plotted. The horizontal bars represent the mean of each group ($n = 12$ in the control group, $n = 12$ in VD group). One representative experiment of three is shown. (d) Tumor size measured at day 25 in xenografted mice. Individual tumor sizes are plotted. The horizontal bars represent the mean of each group ($n = 14$ in the control group, $n = 14$ in the DFO group, and $n = 12$ in the DFO + VD group). (e) Serum ferritin and transferrin levels in xenografted mice. 25 d after the engraftment, the mice were euthanized, and serum was collected for biochemical analysis (mean ± SEM). (f) Sections of

of Syk activity downstream VDR activation could participate in cell differentiation induced by iron deprivation agents and it remains to be evaluated.

VD is known to induce myeloid progenitors to differentiate into monocytes. In vitro and ex vivo experiments were promising, but in the first clinical trials in AML and MDS, only partial differentiation was obtained and clinical improvements were modest (Deeb et al., 2007). In addition, symptomatic hypercalcemia limited VD clinical application. Clinical trials using VD analogues, which do not promote hypercalcemia, did not improve patients' prognosis (Koeffler et al., 2005), suggesting that VDR stimulation alone is not sufficient to promote clinical benefit. We show in this paper that iron deprivation could be a new therapeutic approach in AML, and likely in MDS, because it synergizes with VD (low dose). The combination of iron chelators and VD induced both pro-differentiating and antiproliferative effects in leukemia cells from one AML patient, as described in this paper in the form of a case report. This association reduced the rate of blast proliferation and promoted blast differentiation toward monocytes without emergence of hypercalcemia. The patient developed multiple infectious episodes, which were greatly reduced after the initiation of VD and iron chelation combined therapy. In vitro experiments showed that, in addition to its role in monocyte differentiation, the associated therapy promoted expression of genes related to antimicrobial defense such as cathelicidin. Therefore, the early use of iron chelators in AML therapy, in addition to preventing relapses and enhancing time to progression, could act at multiple levels: by preventing red cell transfusion-derived secondary iron overload, by avoiding defective bone marrow reconstitution after allogeneic HSCT, and also by improving patients' immune status (Pullarkat et al., 2008; Pullarkat, 2009).

Because AML incidence increases with age and because the world population is growing older, we propose that the combined therapy would be particularly useful in elderly patients who are not eligible for high dose chemotherapy and bone marrow transplantation. This combined therapy could be also relevant in other diseases involving a deregulation of BM differentiation, such as MDS. Additional clinical studies are needed to validate its efficacy and determine in which patients it will be more beneficial.

MATERIALS AND METHODS

Clinical samples and cell lines. Peripheral blood cells were obtained from AML patients and healthy donors after obtaining their written informed consent (Table S2, additional information) and approval obtained by the Necker and Saint-Louis Hospitals Institutional ethic committees. Peripheral blood was collected at the initial diagnosis before the administration of treatment. Mononuclear cells were separated by Ficoll-hypaque (PAA laboratories) density centrifugation and resuspended in IMDM (Invitrogen) supplemented with 15% FCS (Hyclone), 100 ng/ml stem cell factor (SCF), 10 ng/ml IL-3, and 25 ng/ml FLT3-L (all purchased from R&D Systems). Myelocytic (HL60 and OCI-AML3), monoblastic (THP1 and U937), and promyelocytic (NB4) leukemia cell lines used in the present study were provided by J.M. Cayuela (Hôpital Saint-Louis, Paris, France) and P. Villarese (Hôpital Necker, Paris, France). Cells were cultured in RPMI-1640 medium (Invitrogen) supplemented with 5% FCS and antibiotics.

Cell treatment and proliferation assays. DFX was provided by Novartis. Etoposide (VP16), ATRA, DFO, 25-OH-VD, H_2O_2, $FeCl_3$, NAC, and PDTC were purchased from Sigma-Aldrich. Calcein-AM, DHR123, and DHE were purchased from Invitrogen. The mAb A24 was produced and purified as described previously (Moura et al., 2001). The inhibitors of JNK (SP600125), ERK (PD98059), and p38 (SB203580) were obtained from Santa Cruz Biotechnology, Inc.

For proliferation assays, the HL60 cell line was resuspended in RPMI-1640 medium with 5% FCS, whereas the patient blasts were resuspended in IMDM with 15% BIT 9500 (STEMCELL Technologies Inc.). The cells were plated in triplicate at 2.5×10^4 cells per well in 96-well tissue culture plates (Falcon) in 200 µl of culture medium. Proliferation was measured as described previously (Lepelletier et al., 2007).

Calcein assay for intracellular LIP. LIP was evaluated according to a previously described method (Espósito et al., 2002) with some modifications. In brief, cells were treated with 0.5 µM calcein-AM for 30 min at 37°C. Before being subjected to flow cytometry analysis, cells were treated or not with an excess of cell-permeant iron chelators. The fluorescein channel was used to detect calcein fluorescence. The difference between calcein fluorescence before and after adding cell-permeant iron chelators indicated the relative amount of LIP (Espósito et al., 2002).

Measurement of intracellular ROS. Fluorescence analysis was used to determine the relative levels of ROS in response to various stimuli. ROS levels were detected by FACS analysis. Labeling with cell-permeant redox-sensitive fluorochromes was performed for 30 min at 37°C in the presence of 1 µM DHE or 0.5 µM DHR123, both diluted in 0.5% BSA in HBSS solution (Invitrogen).

Overexpression and silencing of JNK1, JNK2, and c-Jun. For overexpression, pEGFP-C3 (Takara Bio Inc.) expression vectors containing cDNA encoding JNK1 or JNK2 between the HindIII/BamHI sites (provided by T. Herdegen, Institute of Pharmacology, University Hospital Schleswig-Holstein, Kiel, Germany) were used. These proteins were expressed as a GFP fusion protein under the control of human CMV immediate early promoter.

For *C-Jun*, *JNK1*, and *JNK2* gene silencing, artificial miRNA constructs were generated. Four sets of predesigned miR RNAi sequence oligonucleotides for each gene were obtained using BLOCK-iT miR RNAi Select (Invitrogen) and checked to ensure the designed sequences would not target other gene transcripts to avoid any off-target effects. These oligonucleotides were annealed and ligated into the pcDNA6.2-GW/EmGFP-miR vector according to the manufacturer's instructions (Invitrogen) to express the pre-miRNA as an EmGFP fusion under the control of human CMV immediate early promoter. The pcDNA 6.2-GW/EmGFP-miR–negative control plasmid contains a scrambled miRNA insert, which is predicted not to target any known vertebrate gene.

HL60 cells were transfected with the plasmids using a nucleofector (Lonza) as described according to the manufacturer's instructions (usually 40% cells were transfected). 5 µM DFO was added in culture medium 48 h after transfection and flow cytometry analysis was realized 24 h later on the

tumors from mice injected with vehicle, DFO, and DFO + VD were stained by HE, TUNEL, or labeled with CD11b-, p-ERK– or p-JNK–specific antibodies. The arrows indicate apoptosis. Representative photos of one experiment are shown. Data were quantified using Image J software. Bar, 50 µm. Histograms represent quantification of at least four different fields. One representative experiment is shown (mean ± SEM). *, $P < 0.05$; **, $P < 0.01$; ***, $P < 0.001$.

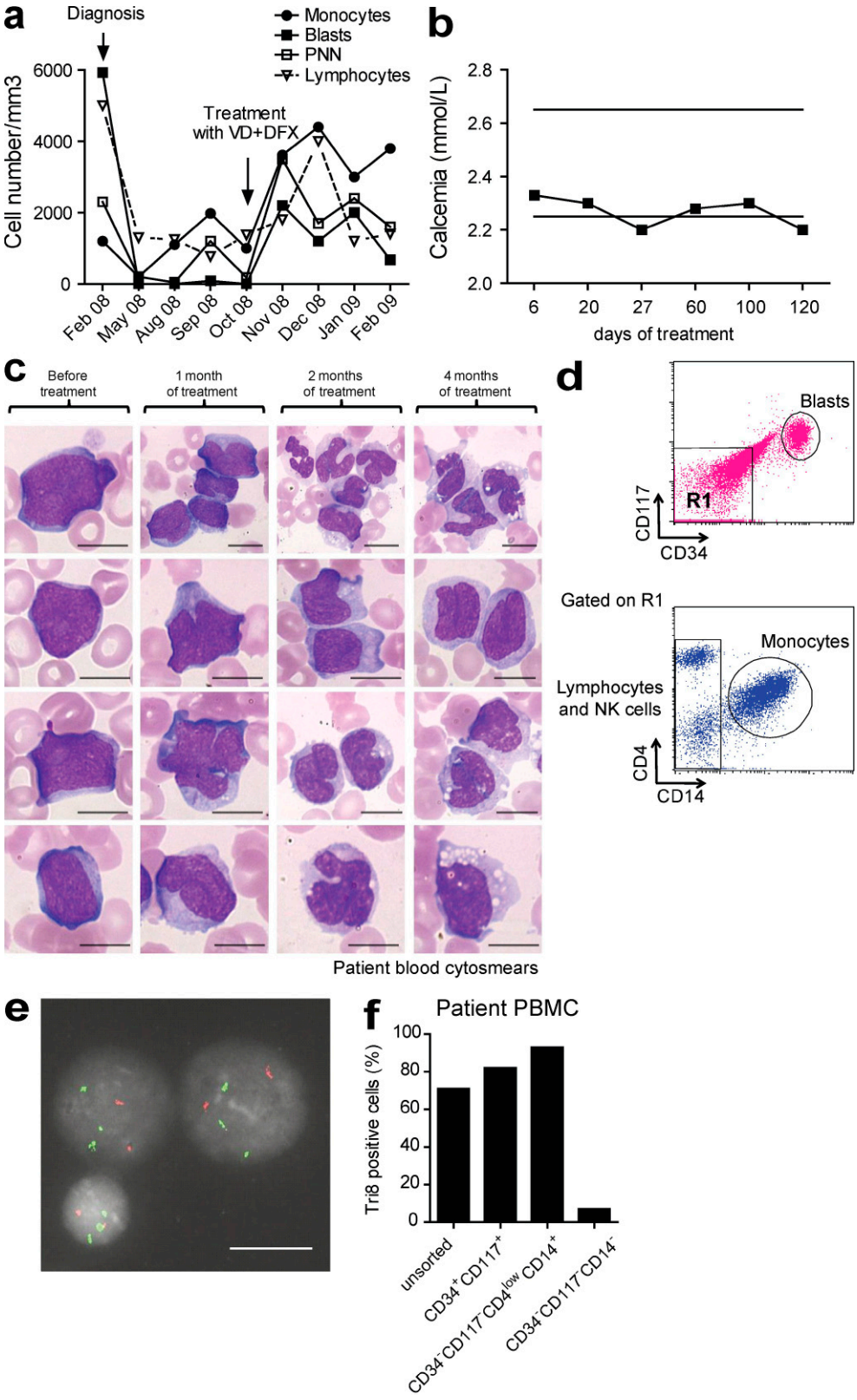

Figure 9. Iron chelation therapy in combination with VD treatment induced blast differentiation in a refractory AML/MDS patient.
(a) Curves representing the blood counts during treatment. The diagnosis and the beginning of the combination therapy are represented with arrows. (b) Plasma calcium concentration during the treatment. Horizontal bars represent minimal and maximal physiological levels of calcemia. (c) MGG-stained blood cytosmears during treatment. At diagnosis, undifferentiated blasts were predominantly observed in MGG-stained blood cytosmears. 1 mo after

basis of the EmGFP (for miRNA) or EGFP (for protein constructs) expression. Validation of miRNA constructs was performed on CHO cells electroporated with each miRNA-containing plasmid using the nucleofector and analyzed in Western blotting after 24 h to validate the constructs.

Cytogenetic analysis. FISH was performed using standard protocols with specific centromeric probes for chromosome 8 (pZ8.4) and chromosome 12 (pBR12; provided by M. Rocchi, University of Bari, Bari, Italy) used as control.

RNA isolation, real-time quantitative PCR, and transcriptome analysis. Total RNA from time-matched controls and treated samples was extracted using NucleoSpin RNA II (Macherey-Nagel). After DNase treatment, first-strand cDNA was synthesized using SuperScript II reverse transcription (Invitrogen). Quantitative real-time PCR was performed using a Chromo-IV PCR System (MJ Research), and the PCR products were quantified using Sybr Green Technology (Jumpstart MasterMix; Sigma-Aldrich). The results of the real-time quantitative PCR were analyzed using the delta-delta Ct method (Livak and Schmittgen, 2001). The complete list of primer sequences is available in Table S4.

For the microarrays, the Agilent 44 K Whole Human Genome (G4112A) long (60 bp) oligonucleotide microarray and the dual-color analysis method were used with probes from the treated samples and from reference RNA that were differentially labeled with cyanine 5 and cyanine 3. These microarrays have 44,290 features with 41,000 distinct oligonucleotides belonging to 33,715 sequences defined by their accession number. cRNA from each treated sample was labeled with Cy3-cytidine triphosphate (CTP) and the untreated HL60 RNA reference pool with Cy5-CTP for direct comparison. Reverse transcription, linear amplification, cRNA labeling, and cRNA purification were performed with the linear amplification kit (Agilent Technologies). The microarray data were mainly analyzed with the Resolver software (Merck). All data were filtered to eliminate low-intensity values <50 arbitrary units for both colors. The microarray data analyzed in this paper have been submitted to the Array Express data repository at the European Bioinformatics Institute (http://www.ebi.ac.uk/arrayexpress/) under accession no. E-TABM-925.

Tumor xenografts. For tumor establishment, 5×10^6 HL60 or 2.5×10^6 OCI-AML3 cells were mixed with Matrigel (1:1, vol/vol) and injected subcutaneously into 8–10-wk-old female athymic Nude mice. The mice were then injected i.p. with A24 (40 mg/kg on day 1), DFO (20 mg/day, 5–7×/wk), VD (1 µg, 2×/wk), and the combination of DFO and VD or PBS as a vehicle control. The tumor growth was measured as previously described (Lepelletier et al., 2007).

Immunohistochemistry. Serial sections (3 µm) in paraffin blocks were deparaffinized in xylene and hydrated in a graded series of alcohol. Staining was performed using the Immunohistochemical Autostainer (Laboratory Vision Corporation) with primary antibodies against CD11b (Sigma-Aldrich, 1:200), p-ERK, and p-JNK (Cell Signaling Technology, 1:200), biotinylated anti-Ig, and streptavidin-peroxidase. The antibody binding was developed in PBS with 0.05% DAB and 0.003% H_2O_2. Hematoxylin-eosin (HE)–stained sections were used to evaluate cytomorphology and to detect apoptotic cells with condensed nuclei. Apoptosis was assessed by the TUNEL technique according to the manufacturer's instructions (Roche). The images were obtained using a microscope (DM-2000; Leica) equipped with a digital camera (DFC320; Leica) and IM50 software. Data were quantified using Image J software (National Institutes of Health).

Cord blood cell cultures and methylcellulose colony-forming assays. $CD34^+$ cord blood cells were isolated by immunomagnetic separation (Miltenyi Biotec) and cultured in IMDM supplemented with 15% BIT 9500 (Stem Cell Technologies), 100 ng/ml SCF, 10 ng/ml IL-3, 25 ng/ml G-CSF, and 10 ng/ml GM-CSF for myelomonocytic differentiation (all cytokines were purchased from R&D Systems). 10 µg/ml A24, 5 µM DFO, or 3 µM DFX was added iteratively every 3 d in the culture medium.

For colony-forming assays, 10^3 $CD34^+$ cells were plated in quadruplicate in semisolid methylcellulose medium (H4434; Stem Cell Technologies) in the presence or absence of 10 µg/ml A24, 5 µM DFO, or 3 µM DFX. At day 14, colonies containing >50 cells were counted and classified as granulocyte colony (CFU-G), monocyte-macrophage colony (CFU-M), mixed granulocyte-monocyte colony (CFU-GM), or erythroid colony (CFU-E). The colonies were counted by standard criteria in 60-mm gridded scoring dishes with cross marks (Stem Cell Technologies) under an inverted microscope. To verify if iron deprivation leads to an altered formation of myelomonocytic colonies, we represented the ratio between CFU-G and CFU-M in both nontreated and treated groups.

Analysis of cellular differentiation and apoptosis. Cell differentiation was determined by the following criteria: cell morphology was evaluated after MGG staining. Esterase activity was detected using the LEUCOGNOST EST kit (Merck). The expression of CD11b (IM2581U; Beckman Coulter) and CD14 (A07765; Beckman Coulter) was evaluated by flow cytometry (FACSCalibur; BD). Cell death was evaluated using the annexin-V/propidium iodide (PI) double staining kit (BD) according to the manufacturer's instructions.

Immunoblotting. All experiments were made with serum-starved cells (12–16 h) to avoid detection of constitutive phosphorylation induced by growth factors (Wang and Proud, 2007). Whole cell extracts were prepared as described previously (Amir-Moazami et al., 2008). In brief, cell pellets (10^7 cells) were washed twice with PBS and then resuspended in 1 ml of lysis buffer (20 mM Tris-HCl, pH 7.4, 150 mM NaCl, 1 mM EDTA, 1 mM EGTA, 1% Triton X-100, 2.5 mM sodium pyrophosphate, 1 mM h-glycerophosphate, 1 mM Na_3VO_4, 1 mM phenylmethylsulfonyl fluoride, 1 µg/ml leupeptin, and 1 µg/ml aprotinin). The protein concentration was determined using the BCA method (Thermo Fisher Scientific) and an equal amount of SDS sample buffer containing 150 mM Tris-HCl, pH 6.8, 30% glycerol, 3% SDS, 1.5 mg/ml bromophenol blue, and 100 mM DTT was then added to each sample. For immunoblotting, 40 µg of protein was separated in 4–12% or 7% SDS-PAGE and transferred onto a PVDF membrane. The blots were first probed with an anti-phospho protein, p-ERK (Thr202/Tyr204), p-JNK, p-p38 (all from Cell Signaling Technology), or p-VDR (Ab63572; Abcam) antibody. The membranes were stripped, dried, and probed with an antibody against total ERK (Cell Signaling Technology), VDR (Ab39990; Abcam), or HSC70 (sc-71270; Sants Cruz Biotechnology, Inc.). The protein bands were visualized using a chemiluminescence system.

beginning treatment, the blasts started to present signs of monocyte differentiation, such as nuclear deformation, cytoplasm enlargement, and the presence of vacuoles. After 3 mo of treatment, undifferentiated blasts were replaced by monocytoid blasts and pro-monocytes. After 4 mo, some monoblasts were still detected, but mature monocytes were predominantly observed. Representative photos of each blood cytosmears are shown. (d) The differentiation potential of blasts treated with combination therapy was evaluated in circulating cells after 3 mo of treatment. PBMCs were isolated, and the cell populations were sorted as follows: blasts ($CD34^+CD117^+$); monocytes ($CD34^-CD117^-CD4^{low}CD14^+$); and lymphocytes and NK cells ($CD34^-CD117^-CD14^-$). The cells were further processed for cytogenetic analysis. (e) FISH analysis. Representative images of chromosomes 8 (green) and 12 (red) probed by fluorescent in situ hybridization demonstrating the trisomy 8 present in the monocytes. (f) Percentage of trisomy 8–positive cells in sorted fractions from d, demonstrating that the monocytes, but not the lymphocytes and NK cells, originated from the blast pool.

Analysis of combined drug effects. CD14 expression was used to evaluate the combined efficacy of DFO, vitamin D, and mAb A24. In each experiment, HL60 cells were treated with serial dilutions of each agent individually and with a fixed ratio of two agents simultaneously. The results were analyzed using the median effect/CI isobologram method of Chou and Talalay (1984). F(a) is the fraction of cells affected (i.e., $CD14^+$) and f(u) is the fraction of cells unaffected (i.e., $CD14^-$). F is the ratio f(a)/f(u) and D is the drug concentration. Log(F) was plotted against log(D). The dose response is displayed as a linear regression line and the x-intercept correspond to the log(IC50). The CI was defined as follows: $CI = (D)_1/(D_x)_1 + (D)_2/(D_x)_2$, where $(D_x)_1$ and $(D_x)_2$ are the doses required to achieve a given effect level for each drug, i.e., a specified value of f(a). $(D)_1$ and $(D)_2$ are the doses of each drug in a given mixture which gives the same f(a). When CI values are 1, <1, or >1, it may be concluded that summation, synergism, or antagonism, respectively have been observed at the particular level examined. The CI was calculated based on the conservation assumption of mutually nonexclusive drug interactions.

Statistical analysis. The data are expressed as the mean ± SEM. Statistical analyses were performed using Prism 5 software (GraphPad Software, Inc.). We used the Student's *t* test or the Mann-Whitney test to compare two groups, and multigroup comparisons were made using a one-way ANOVA followed by a post-hoc Bonferroni test. We used the Kruskal-Wallis test followed by a post-hoc Dunn test for nonparametric comparisons, where indicated. To compare tumor-free animal curves, the Log-rank test was used. The results were considered statistically significant at a p-value <0.05 (*), <0.01 (**), or <0.001 (***).

Online supplemental material. Fig. S1 shows that iron deprivation induces morphological and phenotypical modifications of monocytic cells related to cellular differentiation. Fig S2 shows that iron deprivation inhibits proliferation and induces differentiation of AML blasts. Fig. S3 shows the in vitro granulocytic cord blood progenitor differentiation system. Fig. S4 shows detection of intracellular LIP and ROS in AML cells. Fig. S5 shows the efficacy of miRNA constructs targeting c-JUN, JNK1, and JNK2. Fig. S6 shows determination of the synergic versus additive effect of the combined DFO/VD and A24/VD therapies on cell differentiation. Fig. S7 shows that A24 and iron chelators do not synergize with ATRA to induce differentiation. Fig. S8 shows the anti-tumor effect of iron deprivation and iron deprivation combined with VD in Nude mice xenografted with AML cell lines. Online supplemental material is available at http://www.jem.org/cgi/content/full/jem.20091488/DC1.

The authors would like to thank the members of the hematology and obstetric units (Necker Hospital and St. Louis Hospital, Paris, France) for collecting patient samples and Dr. T. Herdegen (Institute of Pharmacology, University Hospital Schleswig-Holstein, Kiel, Germany) for JNK1 and JNK2 expression plasmids.

This work is supported by the Fondation pour la Recherche Médicale, Fondation de France, Association Laurette Fugain, Association de la recherche contre le cancer, Institut National de la Santé et de la Recherche Médicale (INSERM)/PNRNU2007, and Novartis grants. This work was also supported by a donation from Cyril Mangin's family and Friends. C. Callens was a recipient of an INSERM Poste d'accueil fellowship.

The authors have no conflicting financial interests.

Submitted: 9 July 2009
Accepted: 5 March 2010

REFERENCES

Abe, E., C. Miyaura, H. Sakagami, M. Takeda, K. Konno, T. Yamazaki, S. Yoshiki, and T. Suda. 1981. Differentiation of mouse myeloid leukemia cells induced by 1 alpha,25-dihydroxyvitamin D3. *Proc. Natl. Acad. Sci. USA.* 78:4990–4994. doi:10.1073/pnas.78.8.4990

Adamson, J.W. 1994. The relationship of erythropoietin and iron metabolism to red blood cell production in humans. *Semin. Oncol.* 21:9–15.

Agramonte-Hevia, J., C. Hallal, C. Garay-Canales, C. Guerra-Araiza, I. Camacho-Arroyo, and E. Ortega Soto. 2003. 1alpha, 25-dihydroxy-vitamin D3 alters Syk activation through FcgammaRII in monocytic THP-1 cells. *J. Cell. Biochem.* 89:1056–1076. doi:10.1002/jcb.10575

Amir-Moazami, O., C. Alexia, N. Charles, P. Launay, R.C. Monteiro, and M. Benhamou. 2008. Phospholipid scramblase 1 modulates a selected set of IgE receptor-mediated mast cell responses through LAT-dependent pathway. *J. Biol. Chem.* 283:25514–25523. doi:10.1074/jbc.M705320200

Bastie, J.N., N. Balitrand, F. Guidez, I. Guillemot, J. Larghero, C. Calabresse, C. Chomienne, and L. Delva. 2004. 1 alpha,25-dihydroxyvitamin D3 transrepresses retinoic acid transcriptional activity via vitamin D receptor in myeloid cells. *Mol. Endocrinol.* 18:2685–2699. doi:10.1210/me.2003-0412

Bennett, J.M., D. Catovsky, M.T. Daniel, G. Flandrin, D.A. Galton, H.R. Gralnick, and C. Sultan. 1976. Proposals for the classification of the acute leukaemias. French-American-British (FAB) co-operative group. *Br. J. Haematol.* 33:451–458. doi:10.1111/j.1365-2141.1976.tb03563.x

Boehrer, S., L. Adès, L. Galluzzi, N. Tajeddine, M. Tailler, C. Gardin, S. de Botton, P. Fenaux, and G. Kroemer. 2008. Erlotinib and gefitinib for the treatment of myelodysplastic syndrome and acute myeloid leukemia: a preclinical comparison. *Biochem. Pharmacol.* 76:1417–1425. doi:10.1016/j.bcp.2008.05.024

Callens, C., I.C. Moura, Y. Lepelletier, S. Coulon, A. Renand, M. Dussiot, D. Ghez, M. Benhamou, R.C. Monteiro, A. Bazarbachi, and O. Hermine. 2008. Recent advances in adult T-cell leukemia therapy: focus on a new anti-transferrin receptor monoclonal antibody. *Leukemia.* 22:42–48. doi:10.1038/sj.leu.2404958

Chaston, T.B., R.N. Watts, J. Yuan, and D.R. Richardson. 2004. Potent antitumor activity of novel iron chelators derived from di-2-pyridylketone isonicotinoyl hydrazone involves fenton-derived free radical generation. *Clin. Cancer Res.* 10:7365–7374. doi:10.1158/1078-0432.CCR-04-0865

Chen, Z., S.J. Chen, and Z.Y. Wang. 1994. Retinoic acid and acute promyelocytic leukemia: a model of targetting treatment for human cancer. *C. R. Acad. Sci. III.* 317:1135–1141.

Chou, T.C., and P. Talalay. 1984. Quantitative analysis of dose-effect relationships: the combined effects of multiple drugs or enzyme inhibitors. *Adv. Enzyme Regul.* 22:27–55. doi:10.1016/0065-2571(84)90007-4

Daniels, T.R., T. Delgado, G. Helguera, and M.L. Penichet. 2006a. The transferrin receptor part II: targeted delivery of therapeutic agents into cancer cells. *Clin. Immunol.* 121:159–176. doi:10.1016/j.clim.2006.06.006

Daniels, T.R., T. Delgado, J.A. Rodriguez, G. Helguera, and M.L. Penichet. 2006b. The transferrin receptor part I: biology and targeting with cytotoxic antibodies for the treatment of cancer. *Clin. Immunol.* 121:144–158. doi:10.1016/j.clim.2006.06.010

Davies, M.J. 2005. The oxidative environment and protein damage. *Biochim. Biophys. Acta.* 1703:93–109.

Deeb, K.K., D.L. Trump, and C.S. Johnson. 2007. Vitamin D signalling pathways in cancer: potential for anticancer therapeutics. *Nat. Rev. Cancer.* 7:684–700. doi:10.1038/nrc2196

Espósito, B.P., S. Epsztejn, W. Breuer, and Z.I. Cabantchik. 2002. A review of fluorescence methods for assessing labile iron in cells and biological fluids. *Anal. Biochem.* 304:1–18. doi:10.1006/abio.2002.5611

Faulk, W.P., B.L. Hsi, and P.J. Stevens. 1980. Transferrin and transferrin receptors in carcinoma of the breast. *Lancet.* 2:390–392.

Fenton, R.H., F.B. Johnson, and L.E. Zimmerman. 1964. The combined use of microincineration and the Prussian blue reaction for a more sensitive histochemical demonstration of iron. *J. Histochem. Cytochem.* 12:153–155.

Ferrero, D., E. Campa, C. Dellacasa, S. Campana, C. Foli, and M. Boccadoro. 2004. Differentiating agents + low-dose chemotherapy in the management of old/poor prognosis patients with acute myeloid leukemia or myelodysplastic syndrome. *Haematologica.* 89:619–620.

Friedman, A.D. 2002. Transcriptional regulation of granulocyte and monocyte development. *Oncogene.* 21:3377–3390. doi:10.1038/sj.onc.1205324

Friedman, A.D. 2007. Transcriptional control of granulocyte and monocyte development. *Oncogene*. 26:6816–6828. doi:10.1038/sj.onc.1210764

Fröhling, S., C. Scholl, D.G. Gilliland, and R.L. Levine. 2005. Genetics of myeloid malignancies: pathogenetic and clinical implications. *J. Clin. Oncol.* 23:6285–6295. doi:10.1200/JCO.2005.05.010

Fu, D., and D.R. Richardson. 2007. Iron chelation and regulation of the cell cycle: 2 mechanisms of posttranscriptional regulation of the universal cyclin-dependent kinase inhibitor p21CIP1/WAF1 by iron depletion. *Blood*. 110:752–761. doi:10.1182/blood-2007-03-076737

Gatter, K.C., G. Brown, I.S. Trowbridge, R.E. Woolston, and D.Y. Mason. 1983. Transferrin receptors in human tissues: their distribution and possible clinical relevance. *J. Clin. Pathol.* 36:539–545. doi:10.1136/jcp.36.5.539

Gemelli, C., C. Orlandi, T. Zanocco Marani, A. Martello, T. Vignudelli, F. Ferrari, M. Montanari, S. Parenti, A. Testa, A. Grande, and S. Ferrari. 2008. The vitamin D3/Hox-A10 pathway supports MafB function during the monocyte differentiation of human CD34+ hemopoietic progenitors. *J. Immunol.* 181:5660–5672.

Gilliland, D.G., C.T. Jordan, and C.A. Felix. 2004. The molecular basis of leukemia. *Hematology (Am Soc Hematol Educ Program)*.80–97.

Hahn, C.K., J.E. Berchuck, K.N. Ross, R.M. Kakoza, K. Clauser, A.C. Schinzel, L. Ross, I. Galinsky, T.N. Davis, S.J. Silver, et al. 2009. Proteomic and genetic approaches identify Syk as an AML target. *Cancer Cell*. 16:281–294. doi:10.1016/j.ccr.2009.08.018

Himes, S.R., D.P. Sester, T. Ravasi, S.L. Cronau, T. Sasmono, and D.A. Hume. 2006. The JNK are important for development and survival of macrophages. *J. Immunol.* 176:2219–2228.

Hmama, Z., D. Nandan, L. Sly, K.L. Knutson, P. Herrera-Velit, and N.E. Reiner. 1999. 1α,25-dihydroxyvitamin D_3–induced myeloid cell differentiation is regulated by a vitamin D receptor–phosphatidylinositol 3-kinase signaling complex. *J. Exp. Med.* 190:1583–1594. doi:10.1084/jem.190.11.1583

Hughes, P.J., E. Marcinkowska, E. Gocek, G.P. Studzinski, and G. Brown. 2009. Vitamin D(3)-driven signals for myeloid cell differentiation-Implications for differentiation therapy. *Leuk. Res.* 10.1016/j.leukres.2009.09.010.

Ji, Y., and G.P. Studzinski. 2004. Retinoblastoma protein and CCAAT/enhancer-binding protein beta are required for 1,25-dihydroxyvitamin D3-induced monocytic differentiation of HL60 cells. *Cancer Res.* 64:370–377. doi:10.1158/0008-5472.CAN-03-3029

Johnson, G.L., and R. Lapadat. 2002. Mitogen-activated protein kinase pathways mediated by ERK, JNK, and p38 protein kinases. *Science*. 298:1911–1912. doi:10.1126/science.1072682

Jurutka, P.W., J.C. Hsieh, S. Nakajima, C.A. Haussler, G.K. Whitfield, and M.R. Haussler. 1996. Human vitamin D receptor phosphorylation by casein kinase II at Ser-208 potentiates transcriptional activation. *Proc. Natl. Acad. Sci. USA*. 93:3519–3524. doi:10.1073/pnas.93.8.3519

Kalyanaraman, B. 2007. Iron signaling and oxidant damage. *Cardiovasc. Toxicol.* 7:92–94. doi:10.1007/s12012-007-0025-1

Kansas, G.S., M.J. Muirhead, and M.O. Dailey. 1990. Expression of the CD11/CD18, leukocyte adhesion molecule 1, and CD44 adhesion molecules during normal myeloid and erythroid differentiation in humans. *Blood*. 76:2483–2492.

Kelly, L.M., and D.G. Gilliland. 2002. Genetics of myeloid leukemias. *Annu. Rev. Genomics Hum. Genet.* 3:179–198. doi:10.1146/annurev.genom.3.032802.115046

Koeffler, H.P., T. Amatruda, N. Ikekawa, Y. Kobayashi, and H.F. DeLuca. 1984. Induction of macrophage differentiation of human normal and leukemic myeloid stem cells by 1,25-dihydroxyvitamin D3 and its fluorinated analogues. *Cancer Res.* 44:5624–5628.

Koeffler, H.P., N. Aslanian, and J. O'Kelly. 2005. Vitamin D(2) analog (Paricalcitol; Zemplar) for treatment of myelodysplastic syndrome. *Leuk. Res.* 29:1259–1262. doi:10.1016/j.leukres.2005.04.003

Le, N.T., and D.R. Richardson. 2004. Iron chelators with high antiproliferative activity up-regulate the expression of a growth inhibitory and metastasis suppressor gene: a link between iron metabolism and proliferation. *Blood*. 104:2967–2975. doi:10.1182/blood-2004-05-1866

Lepelletier, Y., V. Camara-Clayette, H. Jin, A. Hermant, S. Coulon, M. Dussiot, M. Arcos-Fajardo, C. Baude, D. Canionni, R. Delarue, et al. 2007. Prevention of mantle lymphoma tumor establishment by routing transferrin receptor toward lysosomal compartments. *Cancer Res.* 67:1145–1154. doi:10.1158/0008-5472.CAN-06-1962

Lim, B.C., H.J. McArdle, and E.H. Morgan. 1987. Transferrin-receptor interaction and iron uptake by reticulocytes of vertebrate animals—a comparative study. *J. Comp. Physiol. [B].* 157:363–371.

Livak, K.J., and T.D. Schmittgen. 2001. Analysis of relative gene expression data using real-time quantitative PCR and the 2(-Delta Delta C(T)) Method. *Methods*. 25:402–408. doi:10.1006/meth.2001.1262

Lopez-Bergami, P., C. Huang, J.S. Goydos, D. Yip, M. Bar-Eli, M. Herlyn, K.S. Smalley, A. Mahale, A. Eroshkin, S. Aaronson, and Z. Ronai. 2007. Rewired ERK-JNK signaling pathways in melanoma. *Cancer Cell*. 11:447–460. doi:10.1016/j.ccr.2007.03.009

Löwenberg, B., J.R. Downing, and A. Burnett. 1999. Acute myeloid leukemia. *N. Engl. J. Med.* 341:1051–1062. doi:10.1056/NEJM199909303411407

Löwenberg, B., G.J. Ossenkoppele, W. van Putten, H.C. Schouten, C. Graux, A. Ferrant, P. Sonneveld, J. Maertens, M. Jongen-Lavrencic, M. von Lilienfeld-Toal, et al; Dutch-Belgian Cooperative Trial Group for Hemato-Oncology (HOVON); German AML Study Group (AMLSG); Swiss Group for Clinical Cancer Research (SAKK) Collaborative Group. 2009. High-dose daunorubicin in older patients with acute myeloid leukemia. *N. Engl. J. Med.* 361:1235–1248. doi:10.1056/NEJMoa0901409

Martindale, J.L., and N.J. Holbrook. 2002. Cellular response to oxidative stress: signaling for suicide and survival. *J. Cell. Physiol.* 192:1–15. doi:10.1002/jcp.10119

Moura, I.C., M.N. Centelles, M. Arcos-Fajardo, D.M. Malheiros, J.F. Collawn, M.D. Cooper, and R.C. Monteiro. 2001. Identification of the transferrin receptor as a novel immunoglobulin (Ig)A1 receptor and its enhanced expression on mesangial cells in IgA nephropathy. *J. Exp. Med.* 194:417–425. doi:10.1084/jem.194.4.417

Moura, I.C., Y. Lepelletier, B. Arnulf, P. England, C. Baude, C. Beaumont, A. Bazarbachi, M. Benhamou, R.C. Monteiro, and O. Hermine. 2004. A neutralizing monoclonal antibody (mAb A24) directed against the transferrin receptor induces apoptosis of tumor T lymphocytes from ATL patients. *Blood*. 103:1838–1845. doi:10.1182/blood-2003-07-2440

Mueller, B.U., T. Pabst, M. Osato, N. Asou, L.M. Johansen, M.D. Minden, G. Behre, W. Hiddemann, Y. Ito, and D.G. Tenen. 2002. Heterozygous PU.1 mutations are associated with acute myeloid leukemia. *Blood*. 100:998–1007. doi:10.1182/blood.V100.3.998

Napier, I., P. Ponka, and D.R. Richardson. 2005. Iron trafficking in the mitochondrion: novel pathways revealed by disease. *Blood*. 105:1867–1874. doi:10.1182/blood-2004-10-3856

Nasr, R., M.C. Guillemin, O. Ferhi, H. Soilihi, L. Peres, C. Berthier, P. Rousselot, M. Robledo-Sarmiento, V. Lallemand-Breitenbach, B. Gourmel, et al. 2008. Eradication of acute promyelocytic leukemia-initiating cells through PML-RARA degradation. *Nat. Med.* 14:1333–1342. doi:10.1038/nm.1891

Owusu-Ansah, E., and U. Banerjee. 2009. Reactive oxygen species prime *Drosophila* haematopoietic progenitors for differentiation. *Nature*. 461:537–541. doi:10.1038/nature08313

Owusu-Ansah, E., A. Yavari, S. Mandal, and U. Banerjee. 2008. Distinct mitochondrial retrograde signals control the G1-S cell cycle checkpoint. *Nat. Genet.* 40:356–361. doi:10.1038/ng.2007.50

Pullarkat, V. 2009. Objectives of iron chelation therapy in myelodysplastic syndromes: more than meets the eye? *Blood*. 114:5251–5255. doi:10.1182/blood-2009-07-234062

Pullarkat, V., S. Blanchard, B. Tegtmeier, A. Dagis, K. Patane, J. Ito, and S.J. Forman. 2008. Iron overload adversely affects outcome of allogeneic hematopoietic cell transplantation. *Bone Marrow Transplant.* 42:799–805. doi:10.1038/bmt.2008.262

Ravandi, F., A.K. Burnett, E.D. Agura, and H.M. Kantarjian. 2007. Progress in the treatment of acute myeloid leukemia. *Cancer.* 110:1900–1910. doi:10.1002/cncr.23000

Renneville, A., C. Roumier, V. Biggio, O. Nibourel, N. Boissel, P. Fenaux, and C. Preudhomme. 2008. Cooperating gene mutations in acute

myeloid leukemia: a review of the literature. *Leukemia*. 22:915–931. doi:10.1038/leu.2008.19

Ricciardi, M.R., T. McQueen, D. Chism, M. Milella, E. Estey, E. Kaldjian, J. Sebolt-Leopold, M. Konopleva, and M. Andreeff. 2005. Quantitative single cell determination of ERK phosphorylation and regulation in relapsed and refractory primary acute myeloid leukemia. *Leukemia*. 19:1543–1549. doi:10.1038/sj.leu.2403859

Richardson, D., P. Ponka, and E. Baker. 1994. The effect of the iron(III) chelator, desferrioxamine, on iron and transferrin uptake by the human malignant melanoma cell. *Cancer Res*. 54:685–689.

Richardson, D.R., D.S. Kalinowski, S. Lau, P.J. Jansson, and D.B. Lovejoy. 2009. Cancer cell iron metabolism and the development of potent iron chelators as anti-tumour agents. *Biochim. Biophys. Acta*. 1790:702–717.

Roumier, C., S. Lejeune-Dumoulin, A. Renneville, A.S. Goethgeluck, N. Philippe, P. Fenaux, and C. Preudhomme. 2006. Cooperation of activating Ras/rtk signal transduction pathway mutations and inactivating myeloid differentiation gene mutations in M0 AML: a study of 45 patients. *Leukemia*. 20:433–436. doi:10.1038/sj.leu.2404097

Sattler, M., T. Winkler, S. Verma, C.H. Byrne, G. Shrikhande, R. Salgia, and J.D. Griffin. 1999. Hematopoietic growth factors signal through the formation of reactive oxygen species. *Blood*. 93:2928–2935.

Sieweke, M.H., and T. Graf. 1998. A transcription factor party during blood cell differentiation. *Curr. Opin. Genet. Dev*. 8:545–551. doi:10.1016/S0959-437X(98)80009-9

Sieweke, M.H., H. Tekotte, J. Frampton, and T. Graf. 1996. MafB is an interaction partner and repressor of Ets-1 that inhibits erythroid differentiation. *Cell*. 85:49–60. doi:10.1016/S0092-8674(00)81081-8

Srivastava, M.D., and J.L. Ambrus. 2004. Effect of 1,25(OH)2 Vitamin D3 analogs on differentiation induction and cytokine modulation in blasts from acute myeloid leukemia patients. *Leuk. Lymphoma*. 45:2119–2126. doi:10.1080/1042819032000159924

Taghon, T., F. Stolz, M. De Smedt, M. Cnockaert, B. Verhasselt, J. Plum, and G. Leclercq. 2002. HOX-A10 regulates hematopoietic lineage commitment: evidence for a monocyte-specific transcription factor. *Blood*. 99:1197–1204. doi:10.1182/blood.V99.4.1197

Tothova, Z., R. Kollipara, B.J. Huntly, B.H. Lee, D.H. Castrillon, D.E. Cullen, E.P. McDowell, S. Lazo-Kallanian, I.R. Williams, C. Sears, et al. 2007. FoxOs are critical mediators of hematopoietic stem cell resistance to physiologic oxidative stress. *Cell*. 128:325–339. doi:10.1016/j.cell.2007.01.003

Trowbridge, I.S., and D.L. Domingo. 1981. Anti-transferrin receptor monoclonal antibody and toxin-antibody conjugates affect growth of human tumour cells. *Nature*. 294:171–173. doi:10.1038/294171a0

Trowbridge, I.S., and D.A. Shackelford. 1986. Structure and function of transferrin receptors and their relationship to cell growth. *Biochem. Soc. Symp*. 51:117–129.

Wang, Z.Y., and Z. Chen. 2008. Acute promyelocytic leukemia: from highly fatal to highly curable. *Blood*. 111:2505–2515. doi:10.1182/blood-2007-07-102798

Wang, X., and C.G. Proud. 2007. Methods for studying signal-dependent regulation of translation factor activity. *Methods Enzymol*. 431:113–142. doi:10.1016/S0076-6879(07)31007-0

Wang, Q., X. Wang, and G.P. Studzinski. 2003. Jun N-terminal kinase pathway enhances signaling of monocytic differentiation of human leukemia cells induced by 1,25-dihydroxyvitamin D3. *J. Cell. Biochem*. 89:1087–1101. doi:10.1002/jcb.10595

Whitmarsh, A.J., and R.J. Davis. 1999. Signal transduction by MAP kinases: regulation by phosphorylation-dependent switches. *Sci. STKE*. 1999:PE1. doi:10.1126/stke.1999.1.pe1

Whitnall, M., J. Howard, P. Ponka, and D.R. Richardson. 2006. A class of iron chelators with a wide spectrum of potent antitumor activity that overcomes resistance to chemotherapeutics. *Proc. Natl. Acad. Sci. USA*. 103:14901–14906. doi:10.1073/pnas.0604979103

Zhu, J., V. Lallemand-Breitenbach, and H. de Thé. 2001. Pathways of retinoic acid- or arsenic trioxide-induced PML/RARalpha catabolism, role of oncogene degradation in disease remission. *Oncogene*. 20:7257–7265. doi:10.1038/sj.onc.1204852